1997-08

Performance Analysis of the Wiener Filter with Applications to Underwater Acoustic Signals

Fontes, N. Ruiz

Monterey, California. Naval Postgraduate School

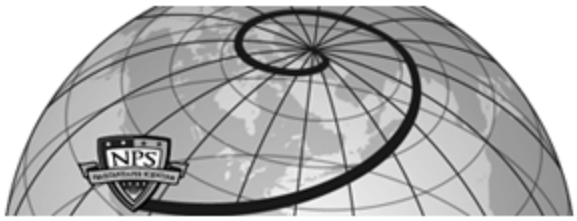

NPS-EC-97-011

NAVAL POSTGRADUATE SCHOOL
Monterey, California

Performance Analysis of the Wiener Filter with Applications to Underwater Acoustic Signals

by

N. Ruiz Fontes
C. W. Therrien

August 1997

Approved for public release; distribution is unlimited.

Prepared **for:** Office of **Naval** Research
800 North **Quincy Street**
Arlington, VA 22217-5000

NAVAL POSTGRADUATE SCHOOL
Monterey, California

Rear Admiral M.J. Evans
Superintendent

R. Elster
Provost

This report was sponsored by the Office of Naval Research.

Approved for public release; distribution is unlimited.

The report was prepared by:

C. W. THERRIEN
Professor
Department of Electrical and
Computer Engineering

Reviewed by:

HERSCHEL H. LOOMIS, JR.
Chairman
Department of Electrical and
Computer Engineering

Released by:

DAVID W. NETZER
Associate Provost and
Dean of Research

REPORT DOCUMENTATION PAGE

Form **Approved**
OMB No. **0704-0188**

1. AGENCY USE ONLY (Leave **blank**)	2. REPORT DATE	3. REPORT TYPE AND DATES COVERED
	August 1997	Final Report FY97

4. TITLE AND SUBTITLE
Performance Analysis of the Wiener Filter with Applications to Underwater Acoustic Signals

5. FUNDING NUMBERS
N6660497WR70391

6. AUTHOR(S)
N. Ruiz Fontes and C. W. Therrien

7. PERFORMING ORGANIZATION NAME(S) AND ADDRESS(ES)
Department of Electrical and Computer Engineering
Naval Postgraduate School
Monterey, CA 93943-5000

8. PERFORMING ORGANIZATION REPORT NUMBER
NPS-EC-97-011

9. SPONSORING/MONITORING AGENCY NAME(S) AND ADDRESS(ES)
Office of Naval Research
800 North Quincy Street
Arlington, VA 22217-5000

10. SPONSORING/MONITORING AGENCY REPORT NUMBER

11. SUPPLEMENTARY NOTES
The views expressed in this report are those of the author and do not reflect the official policy or position of the Department of Defense or the United States Government.

12a. DISTRIBUTION/AVAILABILITY STATEMENT
Approved for public release; distribution is unlimited.

12b. DISTRIBUTION CODE

13. ABSTRACT (Maximum 200 **words)**

This report provides a detailed analysis of the performance of the Wiener optimal filter for estimating **a** signal in additive noise. Both IIR and FIR forms of the filter are considered using a first order *AR* model for both the signal and noise. Expressions are derived for the processing gain, mean-square error and signal distortion, and plotted as a function of the model parameters. **A** more general form of the filter is also presented where one measure of performance, e.g., signal distortion, can be optimized with constraints on the others. Performance on this more general filter is presented **and** compared to that of the Wiener filter.

14. SUBJECT TERMS
noise filtering, Wiener filter, optimal filter, underwater acoustic signals, passive sonar signal processing

15. NUMBER OF PAGES
92

16. PRICE CODE

17. SECURITY CLASSIFICATION OF REPORT	18. SECURITY CLASSIFICATION OF THIS PAGE	19. SECURITY CLASSIFICATION OF ABSTRACT	20. LIMITATION OF ABSTRACT
UNCLASSIFIED	UNCLASSIFIED	UNCLASSIFIED	SAR

TABLE OF CONTENTS

LIST OF FIGURES

PREFACE

The work in this report represents the Masters thesis of LCDR Natanael Ruiz Fontes carried out under the guidance of Professor Charles Therrien of the Naval Postgraduate School.

This work was motivated when Steve Greineder and others of NUWC Code 2121 noticed a significant signal distortion occuring in some cases when a noise cleaning algorithm based on the Wiener filter was applied to some data sets. In addition, certain other questions about performance of the filter, such as the typical processing gain, had been raised and needed some further attention.

Rather than carry out experiments on further empirical data, we decided to take a primarily analytical approach to the problem. In particular, since the answers to these questions concerning the filter is not available in any of the standard literature, we attempted to conduct an investigation of the behavior of the basic Wiener filter and develop formulas by which we could compute the theoretical limits of performance. This was backed up by results on experimental data and would have direct implications for the performance of the noise cleaning algorithm cited above.

The investigation of Wiener filter performance ultimately led to a simple generalization of the filter where various measures of performance could be traded off against each other; so for example, signal distortion could be reduced with some slight overall increase in residual noise and mean-square error.

The formulas in the analysis of the IIR Wiener filter especially, are difficult to derive and some use was made of a symbolic mathematics program to help in the algebraic simplification. Therefore the detailed steps in the derivation are not always presented, but the main formulas and steps are given. The formulas have been checked carefully and verified with experimental results. Several curves and graphs illustrate the results.

I. INTRODUCTION

A. MOTIVATION FOR THE STUDY

Data from passive sonar is generally accompanied by ambient noise arising from shipping traffic, marine life, wave motion, moving or cracking ice (in the Arctic), and numerous other sources. The statistical properties of the noise are variable, even direction-dependent, and have been the source of many studies and analyses [Ref. 1, 2, 3]. Noise degrades sonar data collection and related processing of the data to extract information.

Since ambient noise cannot be completely avoided when collecting real underwater acoustic data, it is desired, in many situations, to remove the noise before further processing. In general, the signals of interest and the ambient noise are non-stationary and their statistics are not known *a priori*. Here we approach the problem of removing additive noise from a given signal by using a *short-time* optimal filtering technique. In this approach we assume that the noise is stationary for the duration of the signal, and that the signal can be assumed stationary over very short time intervals. We exploit this feature and develop improved algorithms for removing the noise.

The work in this report basically consists of two parts. In the first part (Chapters II and III), we perform a detailed analysis of the Wiener filter and evaluate its performance using three different criteria. For this work we use a simple signal model which nevertheless provides insight into results for more general types of signals. Both the IIR and FIR forms of the filter are considered. In the second part (Chapters IV and V), we propose a new algorithm based on a generalization of the Wiener filter and motivated by our analysis, that can be applied to real data. The implementation of the algorithm on a short-time basis is similar to that developed by Frack [Ref. 4] and we use the same basic structure of the programs. Results of the application of this algorithm to underwater acoustic data (biologic data) are presented.

B. PROBLEM DESCRIPTION.

In this section we describe the problem of noise removal to be addressed and introduce the Infinite Impulse Response (IIR) and the Finite Impulse Response (FIR) forms of the Wiener filter used to estimate the signal in noise.

1. Problem Statement.

We consider here the problem of estimating a signal in additive noise. The observed discrete observation sequence is given by

$$x(n) = s(n) + \eta(n) \tag{I.1}$$

where $s(n)$ is the signal and $\eta(n)$ is the noise. The signal duration may be anywhere from a few miliseconds to a few seconds and is generally a nonstationary random process. The noise is assumed to be stationary over the entire observation interval and may be observed without the signal during the early part of the observation interval. That is, the signal becomes non-zero some time after the beginning of the observation interval, and the precise time at which it becomes non-zero is not known. Statistics for the signal and noise, such as mean or correlation function, are not known a *priori* and must be estimated from the data.

Let us assume that the signal is to be estimated by applying the observation sequence to a linear filter as shown in Figure 1, and the filter is designed to minimize the mean-square error

$$\sigma_\epsilon^2 = E\left\{(s(n) - \hat{s}(n))^2\right\}$$

where $\hat{s}(n) = y(n)$ is the filter output. Then the solution for this problem is obtained by solving the Wiener-Hopf equation [Ref. 5], which for the case of a stationary signal has the form

$$\sum_{l=0}^{\infty} R_x(l-i)h[l] = R_{sx}(i); \quad 0 \leq i < \infty \tag{I.2}$$

Here $R_x(l)$ is the correlation function of the observations, $h(l)$ is the impulse response of the filter, and $R_{sx}(l)$ is the cross-correlation function between the signal and the

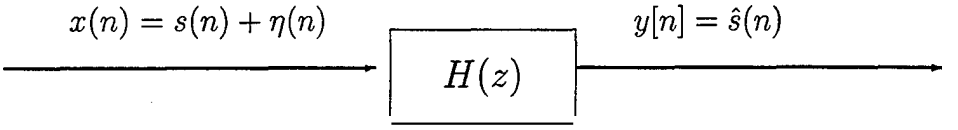

Figure 1. General linear signal estimation problem.

observation sequence. Since the noise is assumed independent of the signal, it is easy to show that

$$R_x(l) = R_s(l) + R_\eta(l) \tag{I.3}$$

and

$$R_{sx}(l) = R_s(l) \tag{I.4}$$

where $R_s(l)$ and $R_\eta(l)$ are the signal and noise correlation functions, respectively. The estimate for the signal is then given by

$$\hat{s}(n) = y(n) = \sum_{k=-\infty}^{n} h(n-k)x(k) \tag{I.5}$$

and the mean-square error can be shown to be

$$\sigma_\epsilon^2 = R_s(0) - \sum_{l=0}^{\infty} h(l)R_{sx}(l) \tag{I.6}$$

where again $R_{sx}(l) = R_s(l)$ for this problem.

When the signal $s(n)$ is nonstationary, as is generally the case in our application, the optimal filter is time-varying and equations (1.2) through (1.6) take on a slightly different form [Ref. 5] involving the time varying correlation functions $R_s(n_1, n_2)$ and $R_x(n_1, n_2)$. Although these correlation functions could be estimated from the data and the corresponding time-varying filter could be computed, it is generally more efficient to take a block-oriented approach where the data is assumed stationary over short segments and the equations for a time-invariant filter are used to find a filter that applies only to the data segment. Although we do not do so in this work, the data segments could be overlapped by some amount, and indeed when the overlap consists of all but the a single

point, the result is equivalent to using the time-varying filter. Thus for purposes of our work and analysis here, (1.2) through (1.6) are the relevant equations.

The Wiener-Hopf equation (1.5) can be solved for two types of filters, the Infinite Impulse Response (IIR) filter, which is applied recursively to the data, and the Finite Impulse Response (FIR) filter, where the filtering process involves a simple convolution. Both of these filters are known as Wiener optimal filters and are described in following sections. Later, we investigate the performance of these two filters in the case when both signal and noise are represented by a first order autoregressive (AR) model. This investigation using a simple model provides insight into the general behavior of the Wiener Filter, and so, helps to predict its behavior for more involved cases.

2. Solution of The Wiener-Hopf Equations: The IIR filter.

The IIR Wiener filter is recursive in form and can have the advantage of requiring fewer parameters than a comparable FIR form of the filter. In many cases the IIR filter is the only true optimal solution to the problem and FIR filters are in fact suboptimal since they do not achieve the absolutely lowest mean-square error. Since the filter is required to be causal, the problem is not straightforward; it was solved (originally in the continuous case) by Wiener using spectral factorization methods [Ref. 6]. Because the solution procedure will be referred to later in this work, we summarize it in this section.

The solution for the IIR filter derives from observing that if the observation sequence is a white noise process $R_x(l) = \sigma_0^2 \delta(l)$ then (1.2) becomes

$$\sum_{l=0}^{\infty} \sigma_0^2 \delta(l-i) h(l) = R_{sx}(i); \quad 0 \le i < \infty \tag{I.7}$$

leading to the simple solution

$$h(l) = \begin{cases} \frac{1}{\sigma_0^2} R_{sx}(l) & l \ge 0 \\ 0 & l < 0 \end{cases} \tag{I.8}$$

The procedure then is to first whiten the observed random process x and then apply the solution above. Thus we conceptually represent the optimal filter h as a cascade of two

filters, the whitening filter g, and the optimal filter h' for the whitened process. Both g and h' are required to be causal.

To find the whitening process we observe [Ref. 5] that the complex spectral density function of the input process x can be factored as

$$S_x(z) = \mathcal{K}_0 H_{ca}(z) H_{ca}(z^{-1}) \tag{I.9}$$

Therefore, if we choose $G(z) = 1/H_{ca}(z)$, we see that the filter g will have the necessary whitening properties and the whitened input process will have variance $\mathcal{K}_0$.

The cross-correlation between the whitened input process and the signal has a complex cross-spectral density function given by $S_{sx}(z)/H_{ca}(z^{-1})$; therefore, the filter corresponding to (1.8) for the whitened process is written as

$$H'(z) = \frac{1}{\mathcal{K}_0}\left[\frac{S_{sx}(z)}{H_{ca}(z^{-1})}\right]_+ \tag{I.10}$$

where the notation $[\,]+$ means that the resulting function corresponds only to the causal part of the quantity within brackets. Finally, by cascading $G(z)$ and $H'(z)$ we obtain the expression for the optimal IIR filter

$$\boxed{H(z) = \frac{1}{\mathcal{K}_0 H_{ca}(z)}\left[\frac{S_{sx}(z)}{H_{ca}(z^{-1})}\right]_+} \tag{1.11}$$

where $H_{ca}(z)$ and $\mathcal{K}_0$ are derived from the spectral factorization (I.9), and $S_{sx}(z)$ is the cross spectral density function for $s(n)$ and $x(n)$.

3. Solution of The Wiener-Hopf Equations: The FIR filter.

The FIR filter is simpler to derive. Since the filter has finite length P, the filtering equation (1.5) can be written as

$$y(n) = \sum_{l=0}^{P-1} h(l)x(n-l) \tag{I.12}$$

We can also directly apply (I.2) noting that the upper and lower limits need to reflect the causality and finite length of the filter. The Wiener-Hopf equation for real process

then becomes

$$\sum_{l=0}^{P-1} R_x(l-i)h(l) = R_{sx}(i); \quad i = 0,1,\ldots,P-1 \tag{1.13}$$

and the mean-square error (1.6) is given by

$$\sigma_\epsilon^2 = R_s(0) - \sum_{l=0}^{P-1} h(l)R_{sx}(l) \tag{I.14}$$

For the FIR filter it is most convenient to write the equations using vector notation. The filter output is written as

$$y[n] = \mathbf{h}^T\tilde{\mathbf{x}} \tag{1.15}$$

where $\mathbf{h}$ and $\tilde{\mathbf{x}}$ are the vectors of filter coefficients and observations respectively

$$\mathbf{h} = \begin{bmatrix} h(0) \\ h(1) \\ \vdots \\ h(P-1) \end{bmatrix} \qquad \tilde{\mathbf{x}} = \begin{bmatrix} x(n) \\ x(n-1) \\ \vdots \\ x(n-P+1) \end{bmatrix}$$

Equations **(1.13)** and **(1.14)** can then be written as

$$\mathbf{R}_x\mathbf{h} = \tilde{\mathbf{r}}_{sx} \tag{1.16}$$

and

$$\sigma_\epsilon^2 = R_s(0) - \mathbf{h}^T\tilde{\mathbf{r}}_{sx} \tag{1.17}$$

where $\mathbf{R}_x = E\left\{\tilde{\mathbf{x}}(n)\tilde{\mathbf{x}}^T(n)\right\}$ and $\tilde{\mathbf{r}}_{sx} = E\{s(n)\tilde{\mathbf{x}}(n)\}$. It follows from (1.3) that

$$\mathbf{R}_x = \mathbf{R}_s + \mathbf{R}_\eta \tag{1.18}$$

where R, and $\mathbf{R}_\eta$ are the signal and noise correlation matrices, and $\tilde{\mathbf{r}}_{sx}$ is the first column of **R,.** This form of the equations is used in the analysis that is presented later in this report.

C. ANALYSIS MODELS.

The detailed analyses presented in this report are based on a first order autoregressive (AR) model for the signal and the noise. The signal $s(n)$ is assumed to be generated according to the difference equation

$$s(n) = \alpha s(n-1) + w_s(n) \tag{1.19}$$

where $w_s(n)$ is a (zero mean) white noise process with variance $\sigma_{w_s}^2$ and α is a real valued parameter with $|\alpha| < 1$. The correlation function for the signal is then found to be

$$R_s(l) = \sigma_s^2 \alpha^{|l|} \tag{1.20}$$

where the signal power σ_s^2 is given by

$$\sigma_s^2 = \frac{\sigma_{w_s}^2}{1-\alpha^2} \tag{1.21}$$

Thus a^l is seen to represent the correlation coefficient for the process $(a = R(1)/R(0))$ with higher values of a^l representing increased correlation. The complex spectral density function for the signal is the z-transform of the correlation function $R_s(l)$ and has the form

$$S_s(z) = \frac{\sigma_s^2 (1-\alpha^2)}{(1-\alpha z)(1-\alpha z^{-1})} \tag{1.22}$$

If this is evaluated on the unit circle $(z = e^{j\omega})$ we have the power spectral density function

$$S_s(e^{j\omega}) = \frac{\sigma_s^2 (1-\alpha^2)}{1+\alpha^2 - 2\alpha\cos(\omega)} \tag{1.23}$$

For $\alpha > 0$ this spectrum has a lowpass character while for $\alpha < 0$ the spectrum has a highpass character (see Figure 2). For $\alpha = 0$ the signal is a white noise sequence and the spectrum is flat.

The noise $\eta(n)$, when it is not white, is represented by a similar model. The noise satisfies the difference equation

$$\eta(n) = \gamma\eta(n-1) + w_\eta(n) \tag{1.24}$$

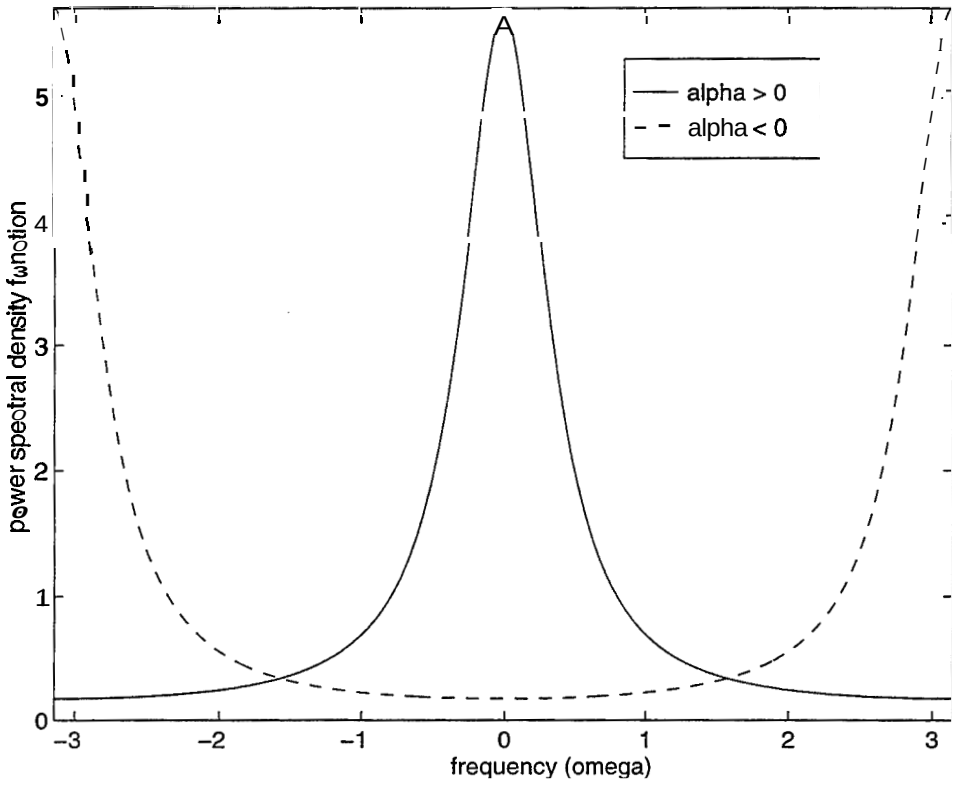

Figure 2. Power spectral density function for real exponential correlation function ($\alpha > 0$ and $a < 0$).

where $w_\eta(n)$ is a white noise process independent of $w_s(n)$, and γ is real with magnitude less than 1. The process has a correlation function of the form

$$R_\eta(l) = \sigma_\eta^2 \gamma^{|l|} \tag{1.25}$$

where the noise power σ_η^2 is given by

$$\sigma_\eta^2 = \frac{\sigma_{w_\eta}^2}{1-\gamma^2} \tag{1.26}$$

and a complex spectral density function

$$S_\eta(z) = \frac{\sigma_\eta^2 \,(1-\gamma^2)}{(1-\gamma z)(1-\gamma z^{-1}} \tag{1.27}$$

The power spectral density function is therefore given by

$$S_\eta(e^{j\omega}) = \frac{\sigma_\eta^2 \,(1-\gamma^2)}{1+\gamma^2 - 2\gamma cos(\omega)} \tag{1.28}$$

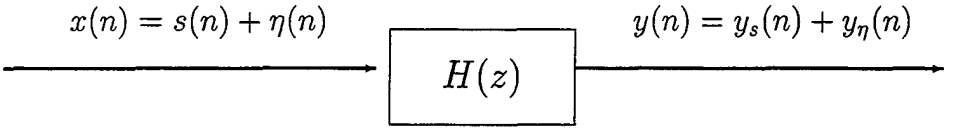

Figure **3.** General linear signal estimation problem.

and has a lowpass or highpass character according to the sign of γ. As described earlier, the noise is assumed to be added to the signal, and the main problem addressed in this report is the removal of the noise or estimation of the signal.

D. FILTERING AND MEASURES OF PERFORMANCE.

We have considered the problem where we observe the sequence $x(n)$ given in **(1.1)** where $s(n)$ is the desired signal and $\eta(n)$ is additive noise uncorrelated with the signal. It is desired to remove as much of the noise as possible by linear filtering. Although we have already discussed the optimal solution in terms of mean-square error, let us temporarily put that solution aside and formulate the problem more generally. We assume that the observed sequence $x(n)$ is applied to a filter and the output of the filter $y(n)$ is an estimate of the signal $s(n)$. Since the filter is linear, we can define components of the output as shown in Figure **3.** In particular $y_s(n)$ is the response of the filter to the signal alone and $y_\eta(n)$ is the response to the noise alone. These components permit defining the following measures of performance:

Processing Gain: The processing gain (PG) for the filter is defined as

$$PG = \frac{\rho_{out}}{\rho_{in}} \tag{1.29}$$

where ρ_{in} and ρ_{out} are the input and output signal-to-noise ratios defined **as**

$$\rho_{in} = \frac{E\{s^2(n)\}}{E\{\eta^2(n)\}} = \frac{R_s(0)}{R_\eta(0)} \tag{1.30}$$

$$\rho_{out} = \frac{E\{y_s^2(n)\}}{E\{y_\eta^2(n)\}} = \frac{R_{y_s}(0)}{R_{y_\eta}(0)} \tag{1.31}$$

The processing gain is usually measured in dB, i.e.,

$$PG(\text{dB}) = 10\log_{10}\frac{Pout}{Pin} \tag{1.32}$$

Processing gain relates to the relative power in the signal and the noise but does not address accuracy of the signal estimate.

Mean Square Error: The mean-square error is the expected value of the squared difference between the signal and the filtered output. Here we use a normalized measure of the mean-square error defined by

$$\text{MSE} = \frac{E\{(s(n) - y(n))^2\}}{E\{s^2(n)\}} = \frac{R_\epsilon(0)}{R_s(0)} \tag{1.33}$$

where $R_\epsilon(l)$ is the correlation function for the "error" defined as $\epsilon(n) = s(n) - \hat{s}(n) = s(n) - y(n)$.

When the output of the filter is equal to the signal itself (except possibly at a countable set of points) then the mean-square error is equal to zero. The maximum occurs when $y(n)$ is zero, where this normalized mean-square error has a value of 1. Mean-square error is the quantity that is optimized in the traditional Wiener optimal filtering problem discussed above.

Signal Distortion: Signal distortion (SD) addresses what the filter does to the signal itself irrespective of the noise, and is defined as

$$\text{SD} = 1 - \frac{E\{s(n)y_s(n)\}^2}{E\{s^2(n)\}\,E\{y_s^2(n)\}} = 1 - \frac{R_{sy_s}^2(0)}{R_s(0)\,R_{y_s}(0)} \tag{1.34}$$

where $R_{sy_s}(l)$ is the cross-correlation function between $s(n)$ and $y_s(n)$. This quantity takes on values in the interval $[0, 1]$ and is minimized when the signal is unchanged by the filter ($y_s(n) = s(n)$), i.e., there is no distortion introduced.

An ideal filter would form a perfect estimate for the signal and completely eliminate the noise. Such a filter would have infinite processing gain, zero mean-square error, and zero signal distortion. Since no linear filter can achieve such ideal performance, we can balance these measures, depending on the application, emphasizing one measure

compared to the others. Thus all of the measures defined above will have use in the sequel.

E. OUTLINE OF REPORT

The remainder of this report is organized as follows. Chapter II introduces, analyses and discusses the performance of the IIR Wiener filter described above. Chapter III provides a similar analysis and discussion of the performance for the FIR form of the Wiener filter. Chapter IV presents a filter based on a new criterion that serves as a generalization of the FIR Wiener filter. This filter, which we call the extended optimal filter, provides a way to improve the signal distortion with only slight degradation in the other performance measures. Chapter V incorporates this technique in a noise removal algorithm based on short term filtering of the observation sequence and demonstrates its performance on sonar data. Chapter VI concludes the report with a summary and suggestions for further investigation.

II. ANALYSIS OF THE IIR WIENER FILTER

In this chapter we derive analytical expressions for the Wiener IIR optimal filter for a signal in colored noise. The signal and the noise are each represented by a first order AR model (equations (1.19) and (1.24)). The expressions for the filter generalize the results obtained in [Ref. 5] which treats the white noise case only.

After deriving an expression for the optimal filter we derive the corresponding expressions for the measures of performance outlined in Chapter I and examine these expressions as a function of some of the parameters describing the model. While the model expressed by (1.19) and (I.24) is only of first order, it exhibits many of the general characteristics of a more complicated model and allows us to draw several general conclusions.

A. THE IIR WIENER FILTER

The general expression for the optimal IIR (Wiener) filter for estimating a real-valued signal $s(n)$ in additive noise $\eta[n]$ (see (1.1))is given by equation (1.11). For the case of a first order AR model, the signal and noise complex spectral density functions are given by (1.22) and (1.27) respectively. Since the signal and noise are independent with zero mean, it follows from (1.4) that the complex spectral density function between the signal $s(n)$ and the observation $x(n)$ is given by

$$S_{sx}(z) = S_s(z) = \frac{\sigma_s^2(1-\alpha^2)}{(1-\alpha z)(1-\alpha z^{-1})} \tag{II.1}$$

Similarly, it follows from (1.3) that the complex spectral density function for the observations is

$$\begin{aligned} S_x(z) &= S_s(z) + S_\eta(z) \\ &= \frac{\sigma_s^2(1-\alpha^2)}{(1-\alpha z)(1-\alpha z^{-1})} + \frac{\sigma_\eta^2(1-\gamma^2)}{(1-\gamma z)(1-\gamma z^{-1})} \\ &= \frac{\sigma_s^2(1-|\alpha|^2)(1+\gamma^2-\gamma z-\gamma z^{-1}) + \sigma_\eta^2(1-|\gamma|^2)(1+\alpha^2-\alpha z-\alpha z^{-1})}{(1-\alpha z^{-1})(1-\alpha z)(1-\gamma z^{-1})(1-\gamma z)} \end{aligned}$$

By collecting terms, this last equation can be written as

$$S_x(z) = \frac{-Az + B - Az^{-1}}{D(z)} \tag{11.2}$$

where

$$A = \gamma\sigma_s^2(1-\alpha^2) + \alpha\sigma_\eta^2(1-\gamma^2) \tag{11.3}$$

$$B = \sigma_s^2(1-\alpha^2)(1+\gamma^2) + \sigma_\eta^2(1-\gamma^2)(1+\alpha^2) \tag{11.4}$$

and

$$D(z) = (1-\alpha z^{-1})(1-\alpha z)(1-\gamma z^{-1})(1-\gamma z) \tag{11.5}$$

After factoring the numerator, we can write (11.2) as

$$S_x(z) = \frac{-Az^{-1}}{D(z)}(z - z_{1a})(z - z_{1b}) \tag{11.6}$$

where

$$z_{1a} = \frac{1}{2}\left(C - \sqrt{C^2 - 4}\right) \tag{11.7}$$

$$z_{1b} = \frac{1}{2}\left(C + \sqrt{C^2 - 4}\right) \tag{11.8}$$

and

$$C = \frac{B}{A} = \frac{\sigma_s^2(1-\alpha^2)(1+\gamma^2) + \sigma_\eta^2(1-\gamma^2)(1+\alpha^2)}{\sigma_s^2(1-\alpha^2)\gamma + \sigma_\eta^2(1-\gamma^2)\alpha} \tag{11.9}$$

This last constant can be expressed as a function of a, γ, and ρ_{in}, as

$$\boxed{C = \frac{[\rho_{in}(1-\alpha^2)(1+\gamma^2)/(1-\gamma^2)] + (1+\alpha^2)}{[\rho_{in}\gamma(1-\alpha^2)/(1-\gamma^2)] + \alpha}} \tag{II.10}$$

where ρ_{in} is the input signal-to-noise ratio

$$\rho_{in} = \frac{\sigma_s^2}{\sigma_\eta^2} \tag{11.11}$$

From the form of the polynomial in (II.2) and (II.6), it can be seen that $z_{1a}z_{1b} = 1$, or that $z_{1b} = 1/z_{1a}$. Let us denote the root that is inside the unit circle in the complex plane as z_1, i.e.,

$$z_1 = \begin{cases} z_{1a} & \text{if } |z_{1a}| < 1 \\ z_{1b} = 1/z_{1a} & \text{otherwise} \end{cases} \tag{11.12}$$

Then from (II.10), we see that z_1 depends only on a, γ, and ρ_{in}.

We can now factor the complex spectral density function $S_x(z)$ by writing it in the form

$$S_x(z) = \frac{A}{z_1} \cdot \frac{(1-z_1z^{-1})}{(1-\alpha z^{-1})(1-\gamma z^{-1})} \frac{(1-z_1z)}{(1-\alpha z)(1-\gamma z)} \tag{11.13}$$

In comparing this with (1.9) we can identify

$$\mathcal{K}_0 = A/z_1 \tag{11.14}$$

and

$$H_{ca}(z) = \frac{(1-z_1z^{-1})}{(1-\alpha z^{-1})(1-\gamma z^{-1})} \tag{11.15}$$

Let us now proceed to compute the term $\left[\frac{S_{sx}(z)}{H_{ca}(z^{-1})}\right]_+$ that appears in (I.11), the equation for the optimal filter. From (11.1) and (II.15), we have

$$\begin{aligned} \frac{S_{sx}(z)}{H_{ca}(z^{-1})} &= \frac{\sigma_s^2(1-|\alpha|^2)}{(1-\alpha z)(1-\alpha z^{-1})} \frac{(1-\alpha z)(1-\gamma z)}{(1-z_1z)} \\ &= \sigma_s^2(1-|\alpha|^2)\frac{\gamma z}{z_1 z} \frac{(1-(1/\gamma)z^{-1})}{(1-\alpha z^{-1})(1-(1/z_1)z^{-1})} \end{aligned}$$

This can be written in a partial fraction expansion as

$$\frac{S_{sx}(z)}{H_{ca}(z^{-1})} = \frac{C_1}{(1-\alpha z^{-1})} + \frac{C_2}{(1-(1/z_1)z^{-1})} \tag{11.16}$$

where

$$C_1 = \sigma_s^2(1-|\alpha|^2)\frac{\gamma}{z_1}\frac{1-(1/\alpha\gamma)}{(1-1/z_1\alpha)} \tag{11.17}$$

and

$$C_2 = \sigma_s^2(1-|\alpha|^2)\frac{\gamma}{z_1}\frac{1-(z_1/\gamma)}{(1-z_1\alpha)} \tag{11.18}$$

The causal part of the expression (11.16) can now be written as

$$H'(z) = \frac{1}{\mathcal{K}_0}\left[\frac{S_{sx}(z)}{H_{ca}(z^{-1})}\right]_+ \tag{11.19}$$

$$= \frac{C_1}{1-\alpha z^{-1}}$$

$$= \frac{z_1}{A}\,\frac{1-1/\alpha\gamma}{1-1/z_1\alpha}\,\frac{\sigma_s^2(1-|\alpha|^2)\,\gamma/z_1}{1-\alpha z^{-1}}$$

$$= \frac{z_1}{A}\,\frac{\alpha-1/\gamma}{\alpha-1/z_1}\,\frac{\sigma_s^2(1-|\alpha|^2)\,\gamma/z_1}{1-\alpha z^{-1}} \tag{11.20}$$

Finally, combining (11.15) and (11.20) we obtain

$$H(z) = \frac{1}{H_{ca}(z)}\,\frac{1}{\mathcal{K}_0}\left[\frac{S_{sx}(z)}{H_{ca}(z^{-1})}\right]_+$$

$$= \frac{(1-\alpha z^{-1})(1-\gamma z^{-1})}{(1-z_1 z^{-1})}\,\frac{z_1}{A}\,\frac{\alpha-1/\gamma}{\alpha-1/z_1}\,\frac{\sigma_s^2(1-|\alpha|^2)\,\gamma/z_1}{(1-\alpha z^{-1})}$$

$$= \left(\frac{z_1}{A}\,\frac{\alpha z_1 - z_1/\gamma}{\alpha z_1 - 1}\,\sigma_s^2(1-|\alpha|^2)\,\gamma/z_1\right)\left(\frac{1-\gamma z^{-1}}{1-z_1 z^{-1}}\right) \tag{11.21}$$

The final expression for the Wiener optimal IIR filter can thus be written as

$$\boxed{H(z) = G\,\left(\frac{1-\gamma z^{-1}}{1-z_1 z^{-1}}\right)} \tag{II.22}$$

where the gain G is given by

$$\boxed{G = \frac{z_1}{A}\,\frac{\alpha\gamma - 1}{\alpha z_1 - 1}\,\sigma_s^2(1-|\alpha|^2)}. \tag{11.23}$$

It is interesting to note that the filter places a zero at $z = \gamma$ in an attempt to cancel the additive noise. Also, it is important to note that z_1 is just a function of the constant C, and, therefore, through (II.10), it is just a function of the input signal-to-noise ratio ρ_{in}, the signal parameter a, and the noise parameter y.

The following figures show the behavior of the pole z_1 for different situations. In Figure **4,** the input signal-to-noise ratio (ρ_{in}) is fixed, but the signal parameter a, varies from **–1** to **+1.** We have plotted the location of the pole z_1 of the optimal filter for different values of γ (y = 0 represents the white noise case). Notice that when $a, = \gamma$, the filter places the pole at the same location $(z_1 = \mathrm{y})$, since it cannot distinguish the signal form the noise. Also observe that when $a, = \pm 1$, the pole is placed at $z = \mathbf{f1}$, regardless of the value of γ. In Figure 5, the noise parameter γ has a fixed value of 0 corresponding

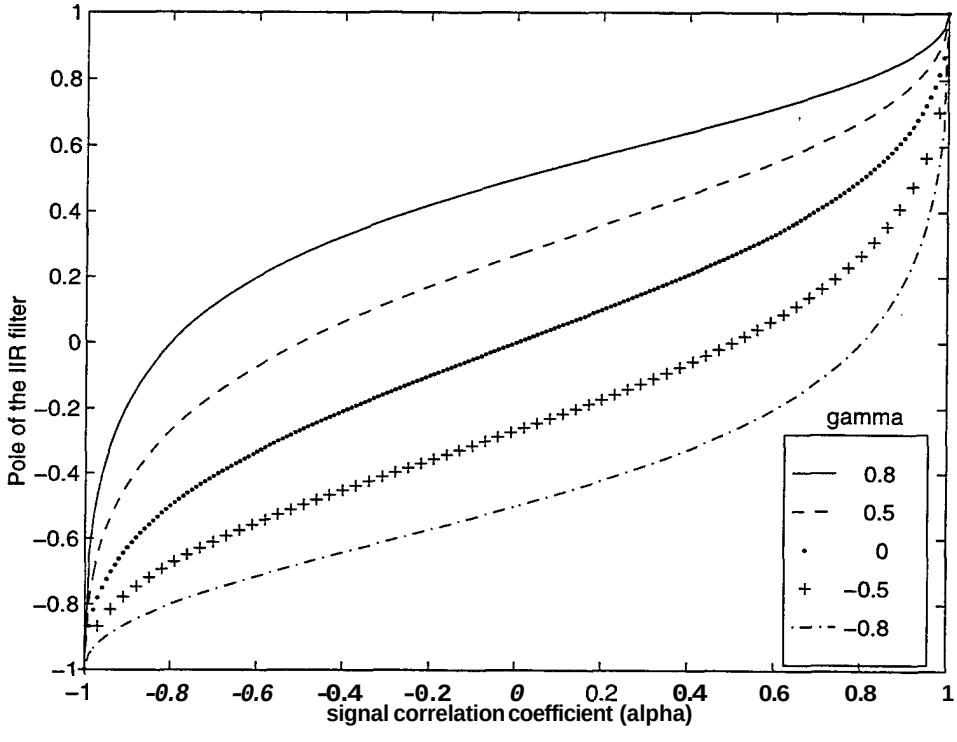

Figure **4.** Location of pole of the IIR filter as a function of signal and noise correlation coefficients $(a,$ and $\gamma)$ for input signal-to-noise ratio of 0 dB.

to white noise, and the pole z_1 is plotted for different values of the input signal-to-noise ratio. Notice in Figure 5 that when the input SNR is small, the pole of the IIR filter approaches the signal parameter α. This can be shown analytically as follows.

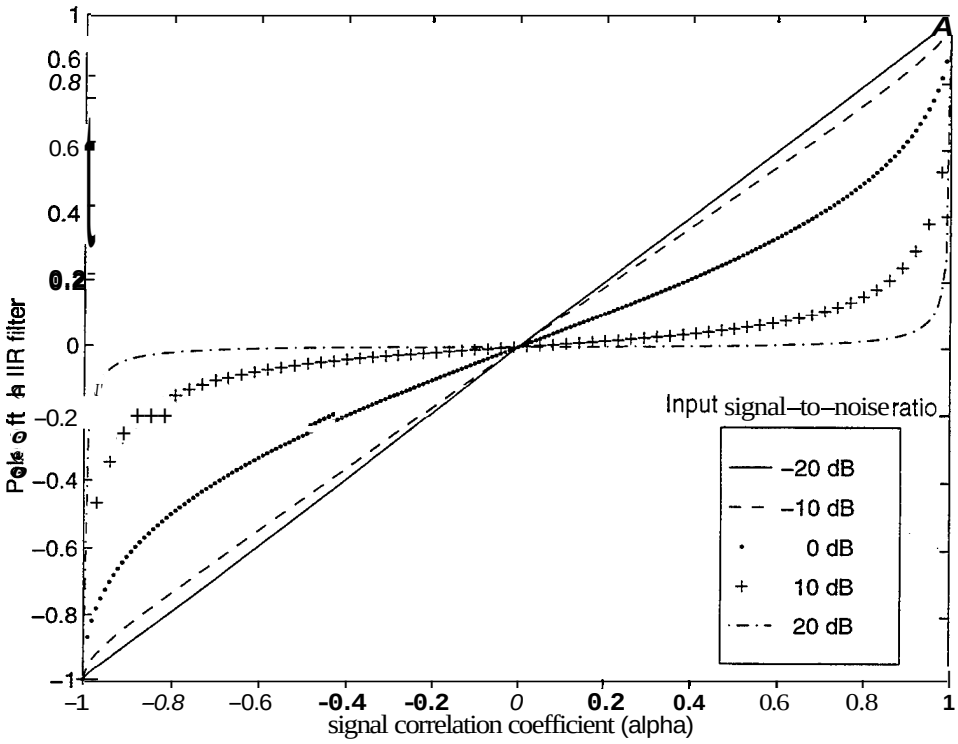

Figure 5. Location of pole of the IIR filter as a function of a for $\gamma = 0$ and different values of the input signal-to-noise ratio.

First, from (11.10) we see that

$$\lim_{\rho_{in}\to 0}(C) = \frac{1+\alpha^2}{\alpha}$$

Thus,

$$\lim_{\rho_{in}\to 0}(z_1) = \frac{1}{2}\left(\frac{(1+\alpha^2)}{\alpha} \pm \sqrt{\frac{(1+\alpha^2)^2 - 4\alpha^2}{\alpha^2}}\right)$$

$$= \frac{1}{2Q}(2\alpha^2) = \alpha \qquad \text{(II.24)}$$

In a similar manner, we can show that for a large input SNR, the pole approaches the noise parameter y. We have

$$\lim_{\rho_{in}\to \infty}(C) = \frac{1+\gamma^2}{\gamma}$$

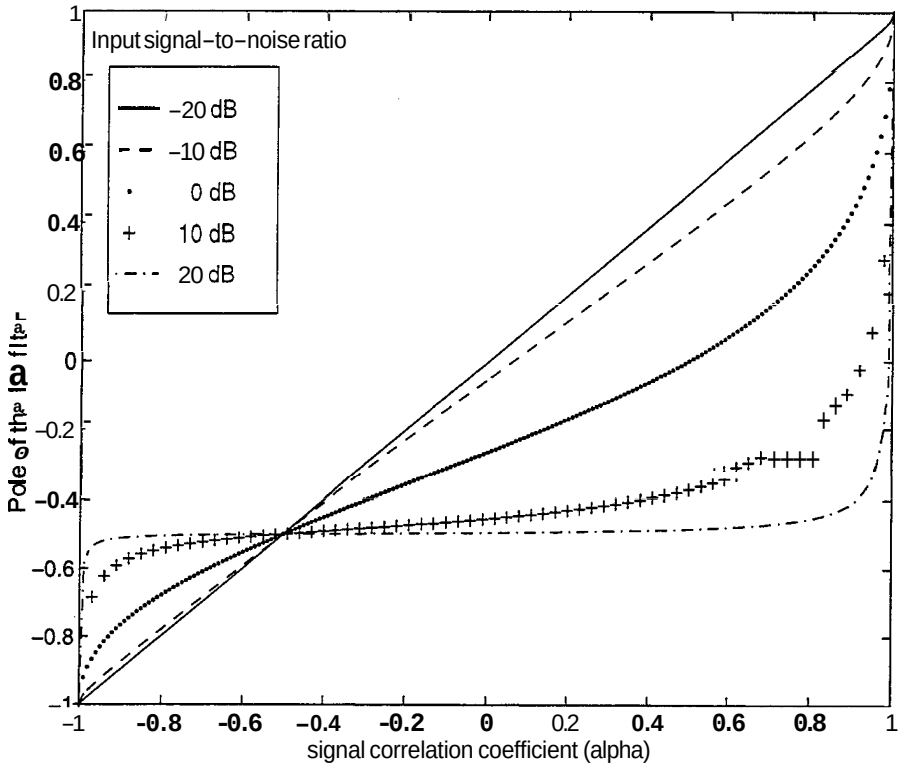

Figure 6. Location of the pole of the IIR filter as a function of α for y $= -0.5$ and different values of the input signal-to-noise ratio.

Therefore

$$\lim_{\rho_{in}\to\infty} z1 = \frac{1}{2}\left(\frac{(1+\gamma^2)}{\gamma} \pm \sqrt{\frac{(1+\gamma^2)^2 - 4\gamma^2}{\gamma^2}}\right)$$
$$= \frac{1}{2\gamma}(2\gamma^2) = \gamma \qquad \text{(II.25)}$$

This characteristic can also be observed in Figure 6, where we have plotted the location of the IIR filter pole as a function of a, for different values of the input signal-to-noise ratio, and for $\gamma = -0.5$. As we will see in a later section, this behavior leads to a better performance, in terms of the processing gain, for smaller values of the input signal-to-noise ratio.

B. PROCESSING GAIN FOR THE IIR FILTER.

Using the first order signal and noise model, we can derive an analytical expression for the processing gain (1.29) for the IIR Wiener Filter. For this we first need the input and output signal-to-noise ratios. The input signal-to-noise ratio is given by (1.30) or (II.11), while the output signal-to-noise ratio is given by (1.31). Hence, the problem is to find expressions for $R_{y_s}(0)$ and $R_{y_\eta}(0)$ in terms of a, γ, σ_s^2, and σ_η^2. To do this, first observe that the complex spectral density of the output of a linear system is given by [Ref. 5]

$$S_y(z) = H(z)H(z^{-1})S_x(z) \tag{11.26}$$

where $H(z)$ is the filter transfer function and S_x is the complex spectral density function of the input. Since the correlation function is related to the complex spectral density function by the inversion formula

$$\begin{aligned} R_y(l) &= \frac{1}{2\pi j}\oint S_y(z)z^{l-1}dz \\ &= \sum \text{Residues}[S_y(x)z^{l-1}] \end{aligned}$$

where the residues correspond only to the poles within the unit circle, we have

$$\begin{aligned} R_y(0) &= \sum \text{Residues}[S_y(z)z^{-1}] \\ &= \sum \text{Residues}[H(z)H(z^{-1})S_x(z)z^{-1}] \end{aligned} \tag{11.27}$$

To evaluate $R_{y_s}(0)$ we use this formula assuming that the input complex spectral density function $S_x(z)$ is that of the signal. Thus from (II.26), (I.22), and (11.22) we obtain

$$S_{y_s}(z)z^{-1} = G^2\frac{1}{z}\frac{1-\gamma z^{-1}}{1-z_1z^{-1}}\frac{1-\gamma z}{1-z_1z}\frac{\sigma_s^2(1-\alpha^2)}{(1-\alpha z^{-1})(1-\alpha z)} \tag{11.28}$$

and, according to (11.27) we have

$$R_{y_s}(0) = \text{RES}_{z=z_1} + \text{RES}_{z=\alpha} + \text{RES}_{z=0} \tag{11.29}$$

where the three residues are given by

$$\text{RES}_{z=z_1} = \frac{G^2(1-\gamma z^{-1})(1-\gamma z)\sigma_s^2(1-\alpha^2)}{(z-z_1)(1-z_1z)(1-\alpha z)(1-\alpha z^{-1})}(z-z_1)\Big|_{z=z_1}$$

$$= \frac{G^2\sigma_s^2(1-\alpha^2)(1-\gamma/z_1)(1-\gamma z_1)}{(1-z_1^2)(1-\alpha/z_1)(1-\alpha z_1)}$$

$$\text{RES}_{z=\alpha} = \frac{G^2(1-\gamma z^{-1})(1-\gamma z)\sigma_s^2(1-\alpha^2)}{(1-z_1 z^{-1})(1-z_1 z)(1-\alpha z)(z-a)}(z-\alpha)\Big|_{z=\alpha}$$

$$= \frac{G^2\sigma_s^2(1-\gamma/\alpha)(1-\gamma\alpha)}{(1-z_1/\alpha)(1-z_1\alpha)}$$

$$\text{RES}_{z=0} = \frac{G^2(1-\gamma z^{-1})(1-\gamma z)\sigma_s^2(1-\alpha^2)z}{z(1-z_1 z^{-1})(1-z_1 z)(1-\alpha z)(1-\alpha z^{-1})}(z-z_1)\Big|_{z=0} = 0$$

Thus combining these results, we have

$$R_{y_s}(0) = \sigma_s^2 G^2\left[\frac{(1-\gamma/z_1)(1-\gamma z_1)(1-\alpha^2)}{(1-z_1^2)(1-\alpha/z_1)(1-\alpha z_1)} + \frac{(1-\gamma/\alpha)(1-\gamma\alpha)}{(1-z_1/\alpha)(1-z_1\alpha)}\right] \tag{II.30}$$

In a similar manner we see that the output complex spectral density due to the noise alone is

$$S_{y_\eta}(z) = G^2 \cdot \frac{1-\gamma z^{-1}}{1-z_1 z^{-1}} \cdot \frac{1-\gamma z}{1-z_1 z} \cdot \frac{\sigma_\eta^2(1-\gamma^2)}{(1-\gamma z^{-1})(1-\gamma z)}$$

$$= G^2\bar{\sigma}_\eta^2 \frac{(1-\gamma^2)}{(1-z_1 z^{-1})(1-z_1 z)} \tag{11.31}$$

Applying (11.27) and evaluating the expression at the single pole $z = z_1$ then leads to

$$R_{y_\eta}(0) = \sigma_{w_\eta}^2 G^2 \frac{1}{(1-z_1^2)} \tag{11.32}$$

By taking the ratio of (11.30) and (11.32) we compute the output signal-to-noise ratio

$$\rho_{out} = \frac{(1-\gamma/z_1)(1-\gamma z_1)}{(1-\alpha/z_1)(1-\alpha z_1)} + \frac{(1-\gamma/\alpha)(1-\gamma\alpha)(1-z_1^2)}{(1-z_1/\alpha)(1-z_1\alpha)(1-\alpha^2)} \tag{II.33}$$

Finally, by substituting (11.11) and (11.33) into the definition (1.29) we obtain the final expression for the processing gain as

$$\boxed{PG = \left[\frac{(1-\gamma/z_1)(1-\gamma z_1)}{(1-\alpha/z_1)(1-\alpha z_1)} + \frac{(1-\gamma/\alpha)(1-\gamma\alpha)(1-z_1^2)}{(1-z_1/\alpha)(1-z_1\alpha)(1-\alpha^2)}\right]\left[\frac{1-\alpha^2}{1-\gamma^2}\right]} \tag{11.34}$$

Figure 7 shows the theoretical and experimental values of the processing gain for different values of a, and for $\gamma = 0$, representing additive *white* noise, at a signal-to-noise

ratio of 0 dB. Figure 8 shows the same curves, but for $y = -0.5$ (colored noise) at an input signal-to-noise ratio of -10 dB. The experimental curve was obtained by averaging measured results for 10 different trials for each value of a, in order to obtain a smaller curve variance. Notice that there is very good agreement between the theoretical and experimental values.

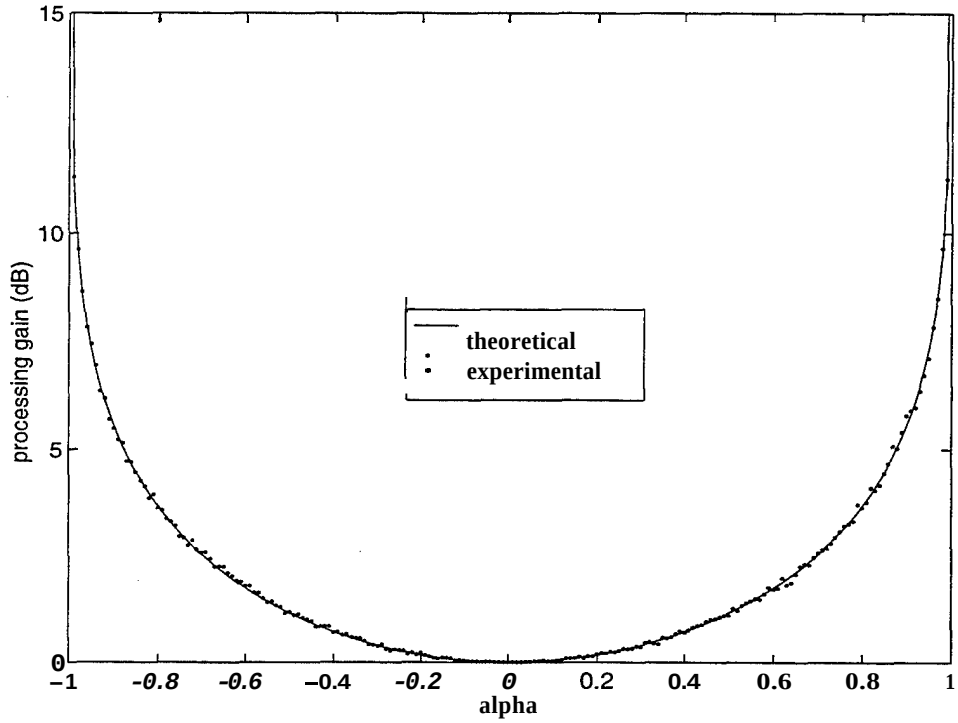

Figure 7. Comparison between theoretical and experimental values of processing gain for the IIR Wiener filter as a function of α, for $y = 0$ (white noise) and input signal-to-noise ratio 0 dB.

Observe from Figures 7 and 8 that the processing gain for the first order IIR filter has its maximum values at $\alpha = \mathbf{f}1$. We can examine the behavior explicitly at these limits as follows. For $a \to \mathbf{f}1$ the constant C in (11.10) approaches ± 2. It follows then

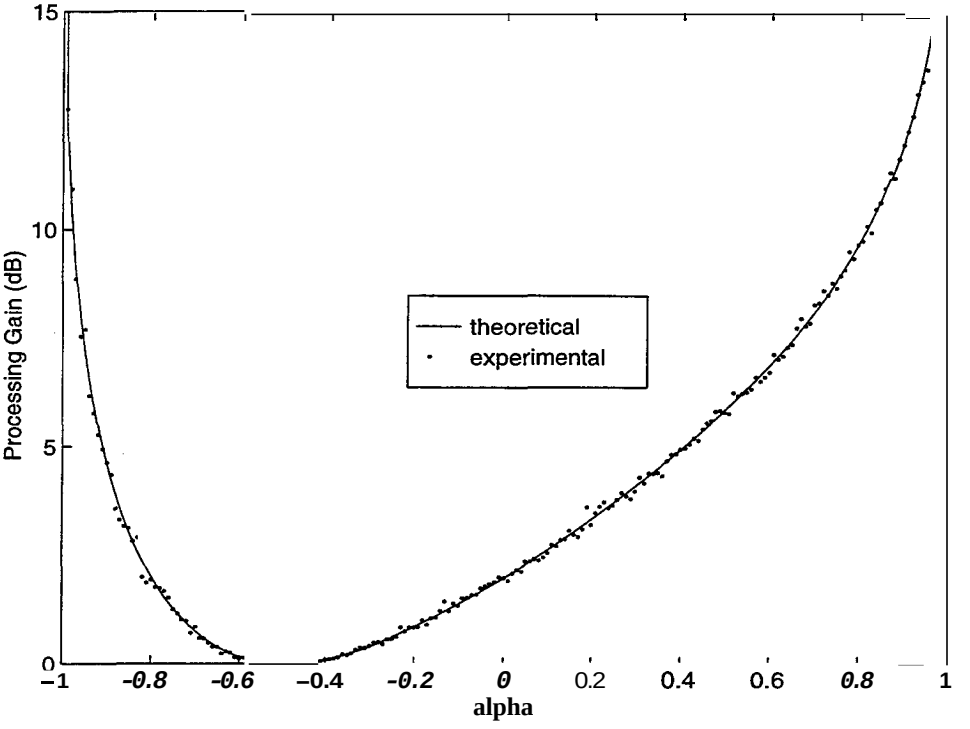

Figure 8. Comparison between theoretical and experimental values of processing gain for the IIR Wiener filter as a function of α, for y $= -0.5$ and input signal-to-noise ratio -10 dB.

from (11.7) and (11.8) that the root z_1 approaches ± 1. Using this result in (11.34) we find

$$\lim_{\alpha \to \pm 1} PG = \frac{(1-\gamma)(1-\gamma)(1-z_1^2)}{(1-z_1)(1-z_1)} \frac{1}{1-\gamma^2} = \frac{(1-\gamma)(1-\gamma)(1-z_1)(1+z_1)}{(1-z_1)(1-z_1)(1-\gamma)(1+\gamma)}$$

$$= \frac{(1-\gamma)(1+z_1)}{(1-z_1)(1+\gamma)} = \infty \tag{11.35}$$

Figures 9 through 11, show the behavior of the processing gain for different values of the input SNR (ρ_{in}), and for $\gamma = 0$, y $= -.5$, and y $= -.999$. Notice that in all of these cases the processing gain approaches infinity as $a! \to \pm 1$. Intuitively, we can see from (11.22) that, for a completely correlated signal $(a! = \pm 1)$, the optimal IIR filter attempts to null the noise (by placing a zero at γ) while completely let the signal pass (pole at $z_1 = \alpha = \pm 1$). Thus, while 'the input signal-to-noise ratio remains finite, the

output signal-to-noise ratio and thus the processing gain becomes infinite.

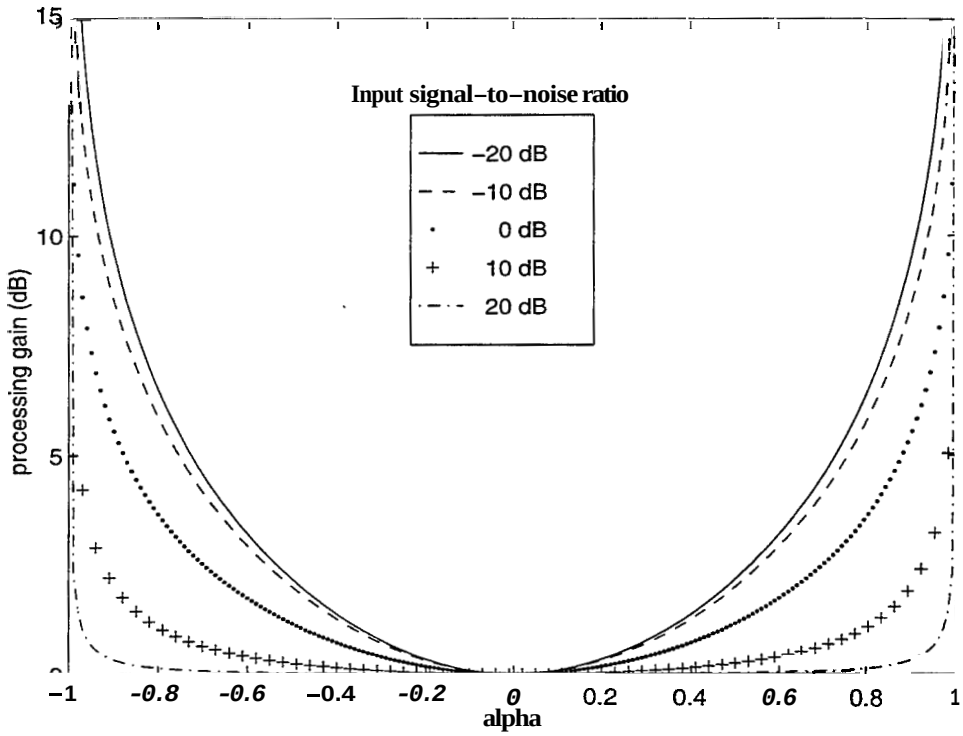

Figure 9. Processing gain for the IIR Wiener filter as a function of α for $\gamma = 0$ and different values of input signal-to-noise ratio.

C. MEAN SQUARE ERROR FOR THE IIR FILTER.

An analytical expression for the mean-square error of the Wiener filter for a first order AR signal in white noise is given in [Ref. 5]. Here we extend that result to the general colored noise case and derive an analytical expression for the MSE given by equation (1.33).

If the error is defined as $\epsilon(n) = s(n) - \hat{s}(n)$, then (1.33) can be written as

$$\text{MSE} = \frac{\sigma_\epsilon^2}{\sigma_s^2} \tag{11.36}$$

where σ_ϵ^2 is the unnormalized mean-square error or error variance. It is shown in [Ref. 5] that the complex cross spectral density function between the signal and the error is

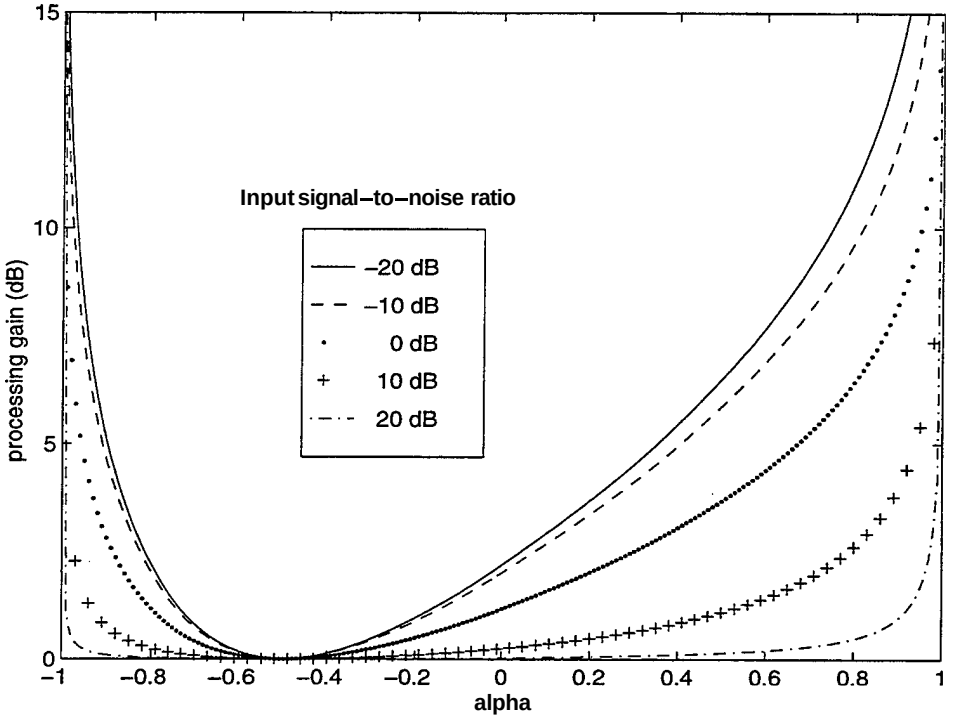

Figure 10. Processing gain for the IIR Wiener filter as a function of α for $\gamma = -0.5$ and different values of input signal-to-noise ratio.

given by

$$S_{s\epsilon}(z) = S_s(z)(1 - H(z^{-1})) \tag{11.37}$$

Substituting (1.22) and (11.22) then yields

$$S_{s\epsilon}(z) = \frac{\sigma_s^2(1-\alpha^2)}{(1-\alpha z)(1-\alpha z^{-1})}\left(1 - G\frac{1-\gamma z}{1-z_1 z}\right) \tag{11.38}$$

By the orthogonality theorem of linear mean-square estimation, the error variance σ_ϵ^2 is equal to the cross-correlation function $R_{s\epsilon}(l)$ evaluated at lag $l = 0$. Therefore from the inversion formula for the complex cross spectral density we have

$$\sigma_\epsilon^2 = R_{s\epsilon}(0) = \frac{1}{2\pi j}\oint S_{s\epsilon}(z)z^{-1}dz \tag{11.39}$$

This integral, involving (11.38) can be evaluated by residues, giving

$$\sigma_\epsilon^2 = \sum \text{Residues}[S_{s\epsilon}(z)z^{-1}]$$

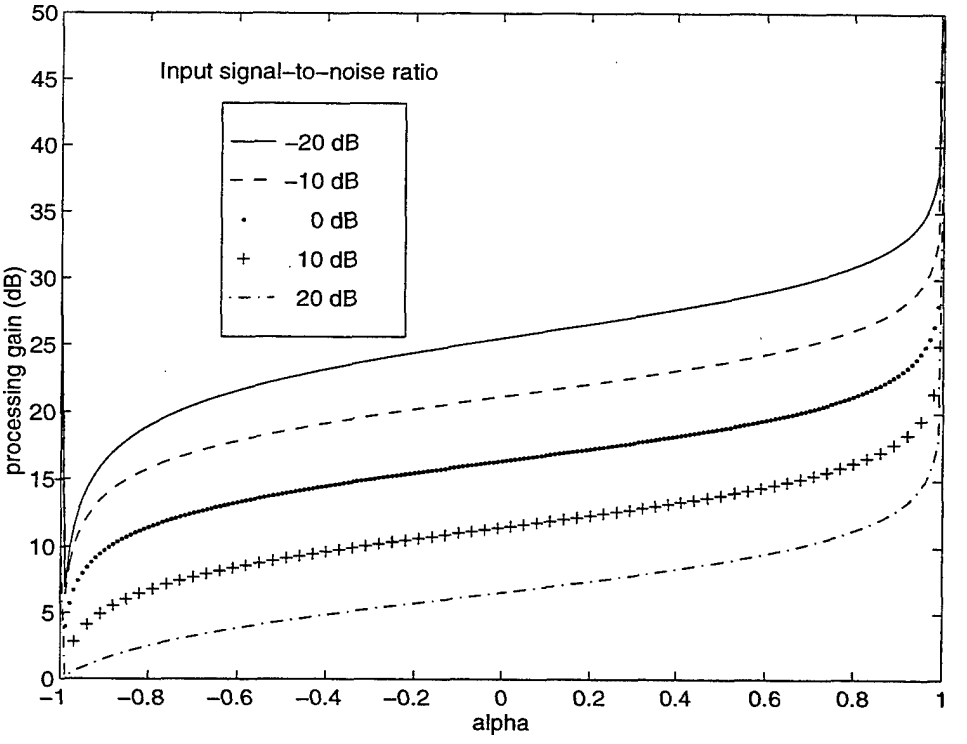

Figure 11. Processing gain for the IIR Wiener filter as a function of a for y $= -.999$ and different values of input signal-to-noise ratio.

$$= \frac{\sigma_s^2(1-\alpha^2)}{(1-\alpha z)(1-\alpha z^{-1})}\left(1 - G\frac{1-\gamma z}{1-z_1 z}\right) z^{-1}\,(z-\alpha)\Big|_{z=\alpha}$$

$$= \sigma_s^2\left(1 - G\frac{1-\gamma\alpha}{1-z_1\alpha}\right)$$

Finally, using this result in (11.36) we obtain

$$\boxed{\text{MSE} = 1 - G\,\frac{(1-\gamma\alpha)}{(1-z_1\alpha)}} \qquad \textbf{(11.40)}$$

Figure 12 compares the theoretical mean-square error for y $= 0$ and $\rho_{in} = 0$ dB with the averaged measured squared errors for the same case. Again, there is a good agreement between the theoretical and the experimental results. Figure 13 shows the behavior of the mean-square error for input signal-to-noise ratio of -10 dB, 0 dB, and 10 dB. Notice that, when $a = \gamma = 0$, MSE $= \sigma_\eta^2/(\sigma_s^2 + \sigma_\eta^2)$. For example, when $\rho_{in} = 0$

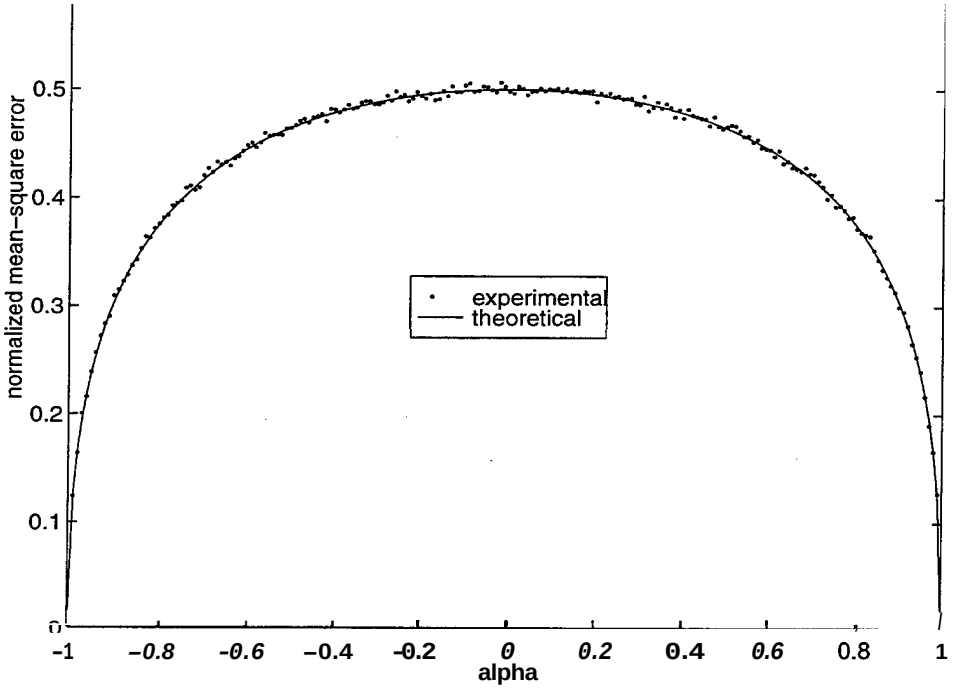

Figure 12. Comparison between theoretical and experimental values of mean square error for the IIR Wiener filter as a function of α for y $= 0$ (white noise) and input signal-to-noise ratio of 0 dB.

dB, the power of the signal equals the power of the noise, and MSE $= 0.5$, as expected. The same analysis for $\rho_{in} = 10$ dB results in MSE $= 0.1/1.1 \approx 0.1$.

Figure 14 shows a case when the noise is not white (y $= -0.5$). The results are qualitatively similar to those for the white noise case. However the curves are skewed, indicating that the worse performance in terms of mean-square error occurs when the signal **has** a correlation coefficient equal to that of the noise.

D. SIGNAL DISTORTION FOR THE IIR FILTER.

In this section we derive an explicit expression for the signal distortion (1.34) produced by the Wiener filter for the problem of a signal in additive noise. As in the previous sections, the signal and the noise are each represented by a first order AR model.

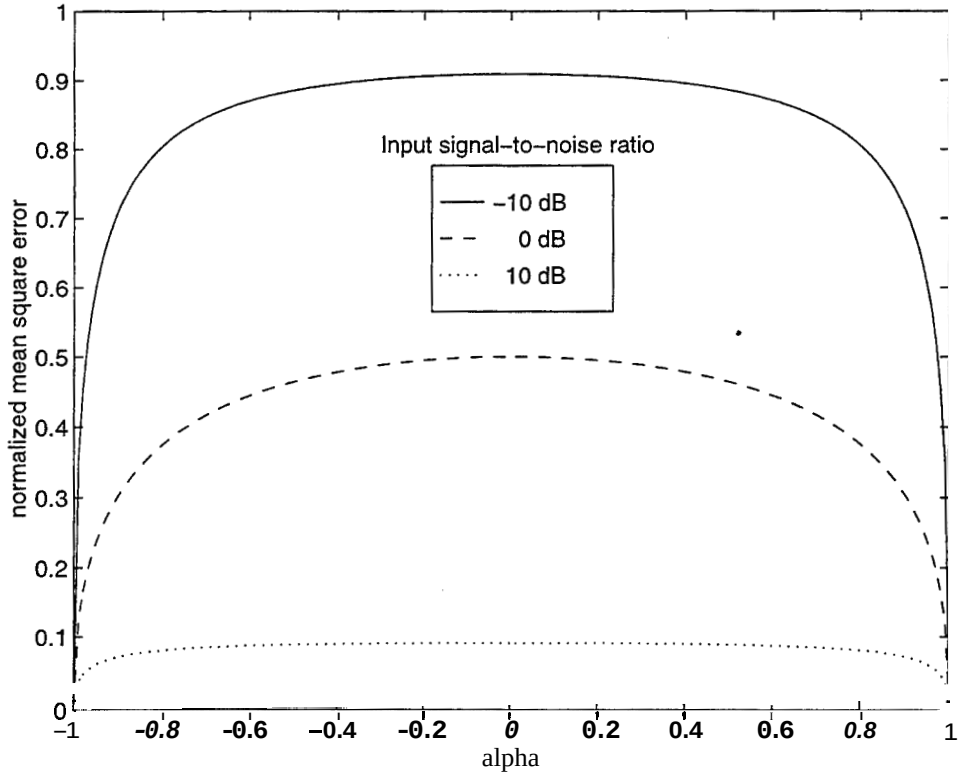

Figure **13.** Mean square error for the IIR Wiener filter as a function of α for $\gamma = 0$ (white noise) and different values of input signal-to-noise ratio.

To evaluate the term $R_{sy_s}(0)$ in (I.34), we begin with the cross complex spectral density function between the input and output of the filter is given [Ref. 5] by

$$S_{sy_s}(z) = H(z^{-1})S_s(z)$$

Therefore, as before, we can evaluate $R_{sy_s}(0)$ from

$$\begin{aligned} R_{sy_s}(0) &= \sum \text{Residues}[S_{y_s}(z)z^{-1}] \\ &= \sum \text{Residues G} \left(\frac{1-\gamma z}{1-z_1 z}\right) \frac{\sigma_s^2(1-\alpha^2)z^{-1}}{(1-\alpha z)(1-ax-1)} \end{aligned} \qquad \text{(II.41)}$$

The only residue is given by

$$\text{Residue} = \text{G} \left.\frac{}{(1-z_1 z)} \sigma_s \frac{}{(1-\alpha z)(1-\alpha z^{-1})z^{-1}(z-a)}\right|_{z=\alpha}$$

(11.42)

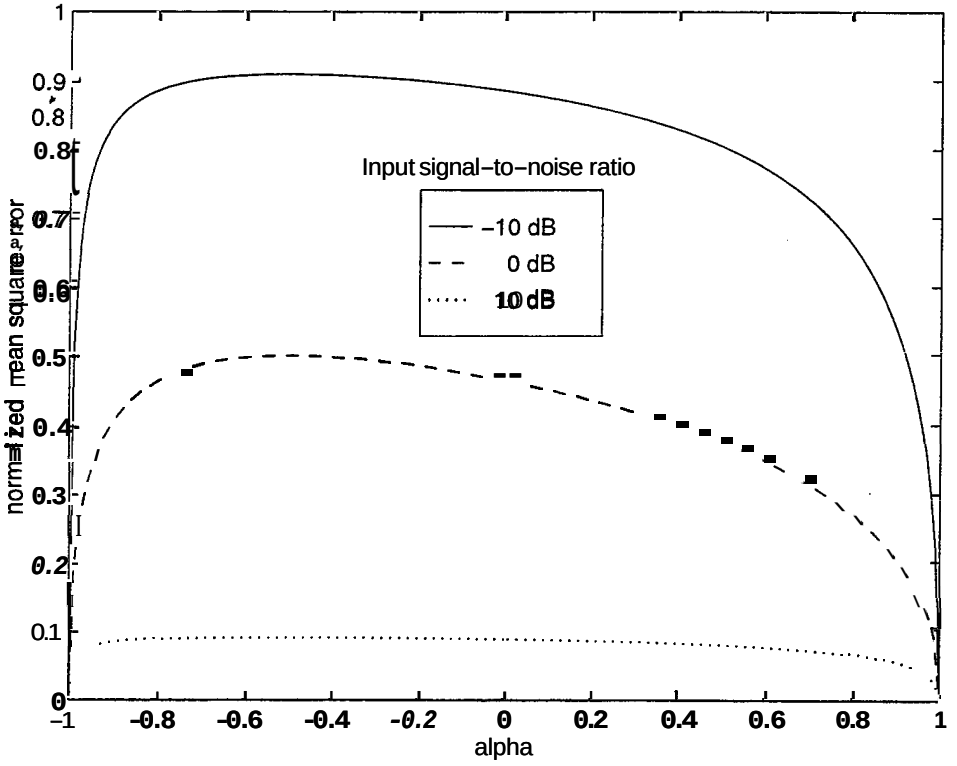

Figure 14. Mean square error for the **IIR** Wiener filter as a function of α for $\gamma = -0.5$ (colored noise) and different values of input signal-to-noise ratio.

resulting in

$$R_{sy_s}(0) = \sigma_s^2 G \frac{(1-\gamma\alpha)}{(1-z_1\alpha)} \tag{11.43}$$

Then, by substituting (II.43), (II.30), and $R_s(0) = \sigma_s^2$ into **(1.34)** we can obtain an expression for signal distortion,

$$SD = 1 - \frac{E}{F} \tag{11.44}$$

where

$$E = \left[\frac{(1-\gamma\alpha)}{(1-z_1\alpha)}\right]^2 \tag{11.45}$$

$$F = \left[\frac{(1-\gamma/z_1)(1-\gamma z_1)(1-\alpha^2)}{(1-z_1^2)(1-\alpha z_1)(1-\alpha/z_1)} + \frac{(1-\gamma/\alpha)(1-\gamma\alpha)}{(1-z_1/\alpha)(1-z_1\alpha)}\right] \tag{II.46}$$

Figure **15** shows the theoretical expression **(11.44)** against the measured results as a function of the correlation factor a, for white noise, with an input signal-to-noise ratio

of 0 dB. Notice that for values of α close to fl, i.e., for highly correlated signals, the distortion is very low. This is also apparent from Figure 16 when the signal distortion

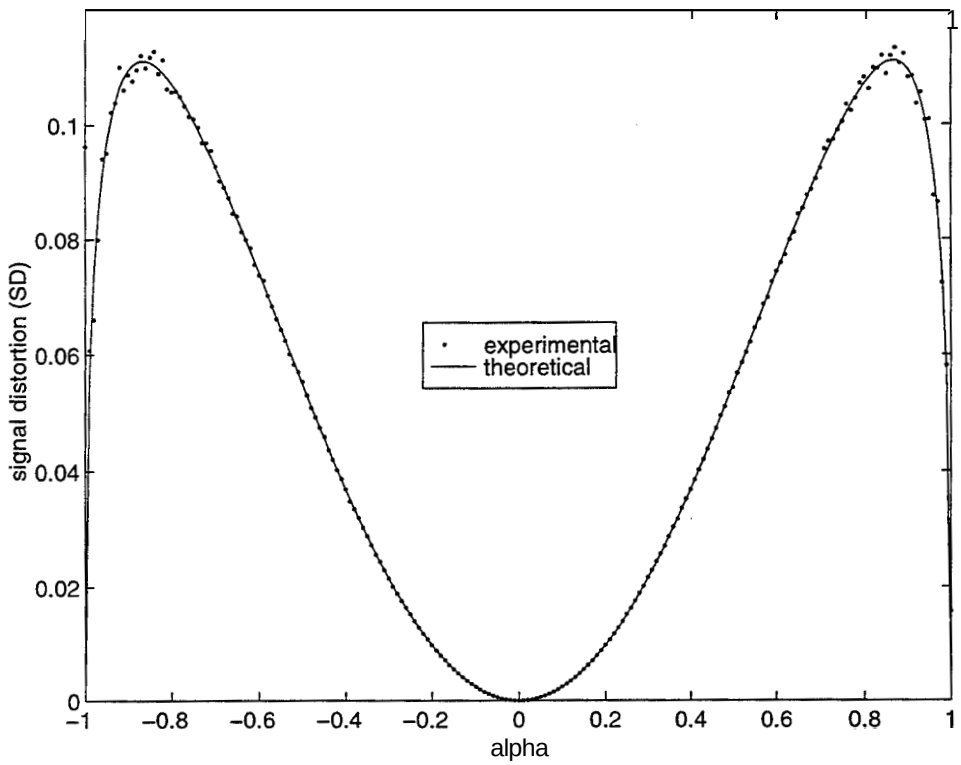

Figure 15. Comparison between theoretical and experimental values of signal distortion for the IIR Wiener filter as a function of α for y $= 0$ and input signal-to-noise ratio 0 dB.

is plotted for several different values of the input signal-to-noise ratio. Figure 16 also shows that the signal distortion is lower for higher values of the input signal-to-noise ratio, because the filter is able to pass more of the signal. Since we already know that $\lim_{\alpha\to 1} z_1 = 1$, we can evaluate the $\lim_{\alpha\to 1}$ for (11.46) and verify that $\lim_{\alpha\to 1} SD = 0$. Also, for $\alpha =$ y (which implies that $H(z)$ is an all-pass filter) the distortion is zero, as expected. However, there is a value for a, which we shall call the critical value α_c, where the distortion reaches its maximum value. This value depends on ρ_{in}.

Figure 17 shows the result for y $= -0.5$. Again the distortion peaks at specific critical values of the correlation coefficient α_c. However, in this case the two values do

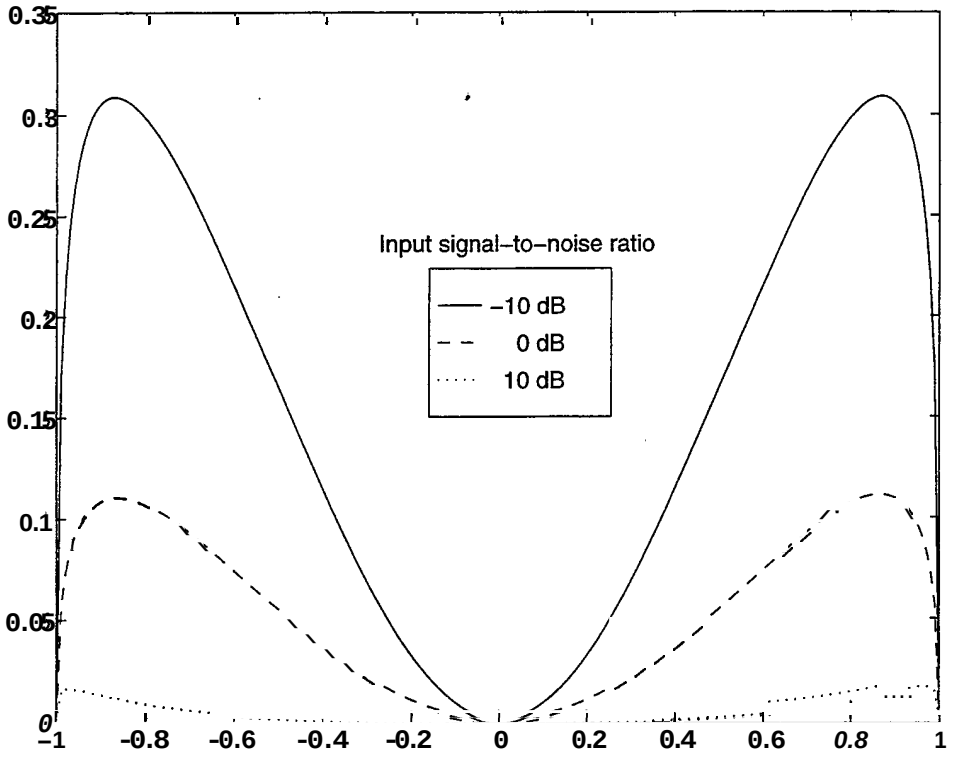

Figure 16. Signal distortion for the IIR Wiener filter as a function of a_1 for y = 0 (white noise) and different values of input signal-to-noise ratio.

not occur at locations symmetrically distributed about the origin.

E. SUMMARY

The analysis of this chapter based on the first order **AR** signal and noise model shows that the optimal filter for estimating the signal is also of first order. The filter has a zero at the location γ corresponding to the noise correlation coefficient, and a pole at location z_1 which moves from -1 to $+1$ as the signal correlation coefficient a_1 moves from -1 to $+1$ (see Figure 5). For low values of the input signal-to-noise ratio the pole z_1 becomes very nearly equal to a_1, while for high input signal-to-noise ratio z_1 approaches γ and the filter becomes an all-pass filter.

The processing gain (PG) for the optimal filter increases with increasing signal correlation and becomes infinity in the limit as α approaches ± 1 (perfectly correlated

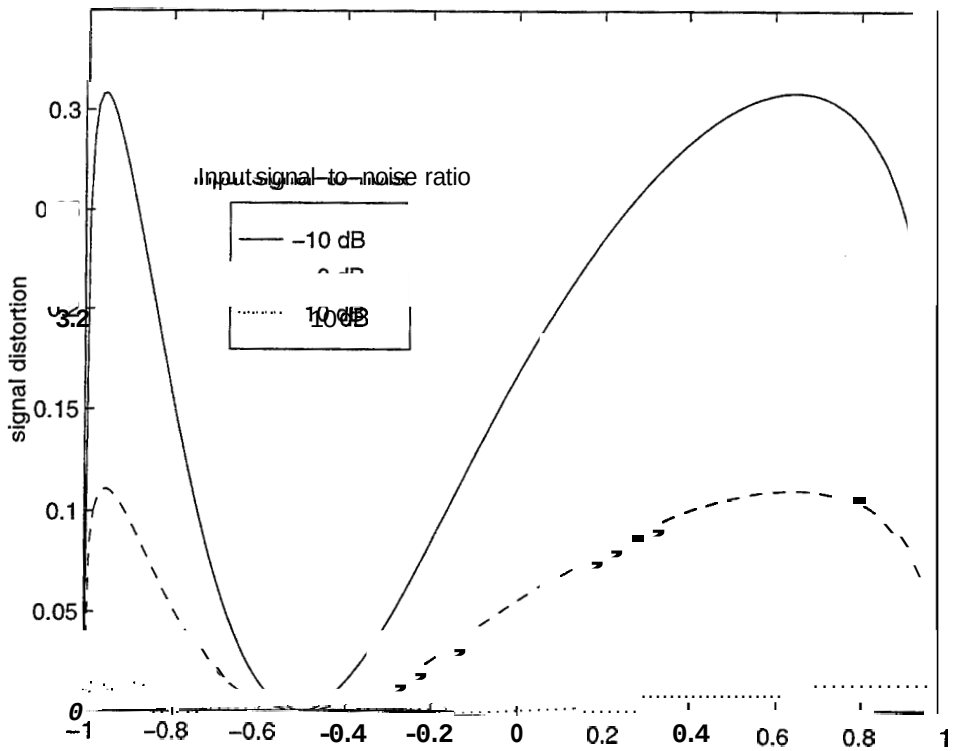

Figure 17. Signal distortion for the IIR Wiener filter as a function of α for y $= -0.5$ (colored noise) and different values of input signal-to-noise ratio.

signal). The processing gain decreases as the input signal-to-noise ratio increases indicating that less improvement is possible when the input signal-to-noise ratio is already high.

The normalized mean-square error (MSE) for the optimal filter decreases with increasing correlation and becomes zero in the limit as α approaches ± 1. It is fairly flat for most values of a and decreases most rapidly as a approaches ± 1. The normalized mean-square error (MSE) also increases when the input signal-to-noise ratio decreases.

The signal distortion (SD) becomes zero when $\alpha = \gamma$, where the filter becomes an all-pass filter, and when α approaches ± 1, where the signal is completely correlated. It achieves its maximum values for moderately high values of correlation. In the case of white noise this occurs around $0.8 < |\alpha_c| < 0.9$. (see Figure 16).

The performance of the filter for colored noise parallels that of the filter for white

noise. However, the symmetry with respect to $a = 0$ is lost. When $a = \gamma$, the processing gain goes to zero, the mean-square error achieves its maximum value, and the signal distortion goes to zero. Maximum values of the signal distortion occur at two distinct points above and bellow the value of the noise correlation parameter γ (see Figure 17).

111. ANALYSIS OF THE FIR WIENER FILTER.

In this chapter we develop expressions for the FIR form of the Wiener filter for the case where the signal and the noise are, again, each represented by a first order AR model (equations (1.19) and (1.24)). The chapter is divided into two parts. In Part A, we derive analytical expressions for the first order FIR Wiener filter, i.e., a FIR filter with only two coefficients. In Part B, we use a more general approach to derive expressions for a filter of any order. Although Part **A** treats a restricted particular case, it allows us to obtain simple expressions for the measures of performance as functions of the model parameters. On the other hand, the results of Part B permit us to plot the measures of performance for more general cases, where the FIR filter can be of any order.

A. THE FIRST ORDER FIR WIENER FILTER.

In Chapter I we introduced the matrix form of the Wiener-Hopf equation (1.16) for the FIR Wiener filter and the associated mean-square error (1.17). For the first order FIR Wiener filter, the vector of filter coefficients h has only two elements, i.e., $\mathrm{h} = [h(0)\ h(1)]^T$. Thus we can obtain expressions for these two coefficients by solving equation (1.16) as follows. Since the noise is assumed uncorrelated with the signal, $R_x(l)$ and $R_{sx}(l)$ are given by (1.3) and (1.4). Evaluating (1.20) and **(1.25)** for lag $l = 0$ and 1, and substituting in **(1.3)** yields

$$R_x(0) = a,'' + a; = \sigma_\eta^2[1 + \rho_{in}] \tag{111.1}$$

and

$$R_x(1) = \sigma_s^2\alpha + \sigma_\eta^2\gamma = \sigma_\eta^2[\gamma + \alpha\rho_{in}] \tag{111.2}$$

Similarly, from (I.20) and (I.4) we obtain

$$R_{sx}(0) = \sigma_s^2 \tag{111.3}$$

and

$$R_{sx}(1) = \alpha\sigma_s^2 \tag{111.4}$$

Using (111.1) through (111.4) in equation (1.16) results in

$$\sigma_\eta^2 \begin{bmatrix} (\rho_{in}+1) & (\alpha\rho_{in}+\gamma) \\ (\alpha\rho_{in}+\gamma) & (\rho_{in}+1) \end{bmatrix} \begin{bmatrix} h(0) \\ h(1) \end{bmatrix} = \sigma_s^2 \begin{bmatrix} 1 \\ \alpha \end{bmatrix}$$

Then, solving this matrix equation by inverting the matrix, we can express the filter coefficients as

$$\begin{bmatrix} h(0) \\ h(1) \end{bmatrix} = \frac{\rho_{in}}{(\rho_{in}+1)^2 - (\alpha\rho_{in}+\gamma)^2} \begin{bmatrix} \rho_{in}+1 & -(\alpha\rho_{in}+\gamma) \\ -(\alpha\rho_{in}+\gamma) & \rho_{in}+1 \end{bmatrix} \begin{bmatrix} 1 \\ \alpha \end{bmatrix}$$

or,

$$\boxed{h(0) = \rho_{in}\frac{(\rho_{in}+1-\alpha^2\rho_{in}-\alpha\gamma)}{(\rho_{in}+1)^2-(\alpha\rho_{in}+\gamma)^2}} \tag{111.5}$$

$$\boxed{h(1) = \rho_{in}\frac{(\alpha-\gamma)}{(\rho_{in}+1)^2-(\alpha\rho_{in}+\gamma)^2}} \tag{111.6}$$

The transfer function for the filter is then given by

$$H(z) = h(0) + h(1)z^{-1}$$

or

$$\boxed{H(z) = h(0)(1 - z_0 z^{-1})} \tag{111.7}$$

where the zero of the filter is located at

$$z = z_0 = -\frac{h(1)}{h(0)} \tag{111.8}$$

or

$$\boxed{z_0 = \frac{(\gamma-\alpha)}{(\rho_{in}+1-\alpha^2\rho_{in}-\alpha\gamma)}} \tag{111.9}$$

Figures 18 and 19 show the location of the zero z_0 of the first order FIR Wiener filter as a function of Q for different values of γ, and for an input signal-to-noise ratio of 0 dB and -10 dB, respectively. From these figures we can identify three interesting cases.

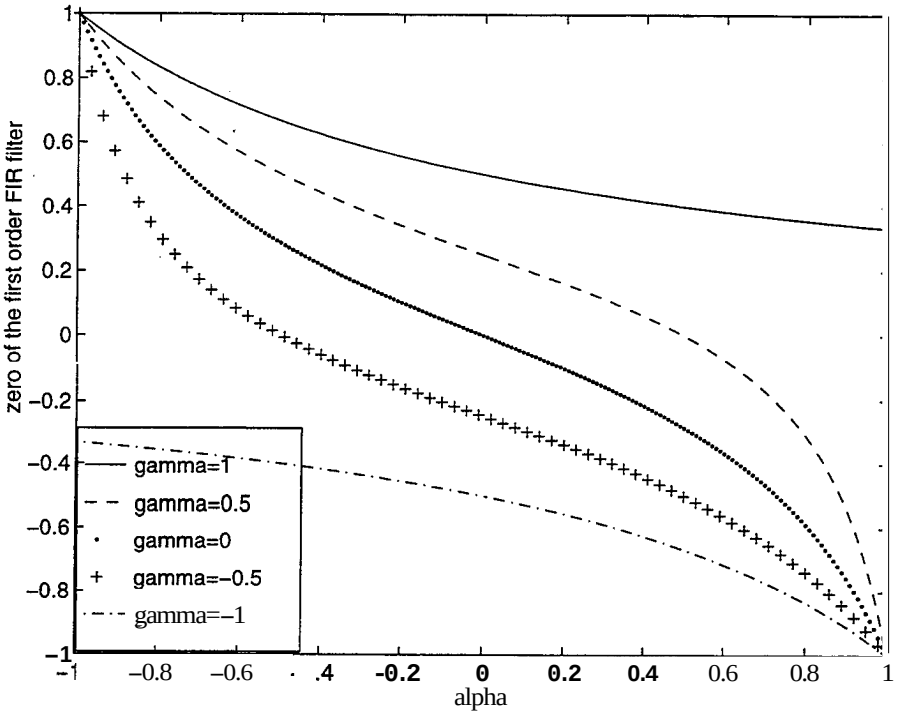

Figure 18. Location of the zero of the first order FIR as a function of the signal and noise correlation coefficients (α and γ) for input signal-to-noise ratio of 0 dB.

First, for $\alpha = \pm 1$ and $\gamma \neq \pm 1$, and any value of the input signal-to-noise ratio, the filter places the zero at $z_0 = \mp 1$. This can be easily verified from equation (111.9). Secondly, when $\alpha = \pm 1$ and y $= \pm 1$ we see that z_0 assumes different values. These values can be found by setting $\gamma = \pm 1$ in (111.9) obtaining

$$z_0 = \frac{\pm 1 - \alpha}{\rho_{in} + 1 - \alpha^2 \rho_{in} \mp \alpha}$$

and evaluating

$$z_0 = \lim_{\alpha \to \pm 1} \frac{\pm 1 - \alpha}{\rho_{in} + 1 - \alpha^2 \rho_{in} \mp \alpha} = \lim_{\alpha \to \pm 1} \frac{-1}{-2\alpha\rho_{in} \mp 1} = \frac{\pm 1}{2\rho_{in} + 1} \qquad (111.10)$$

Finally, when $\alpha =$ y # fl, the filter places the zero at $z_0 = 0$, regardless the value of input signal-to-noise ratio. This seems intuitively correct, since when Q = y the filter cannot distinguish the signal from the noise, and should become an "all pass" filter ($z_0 = 0$).

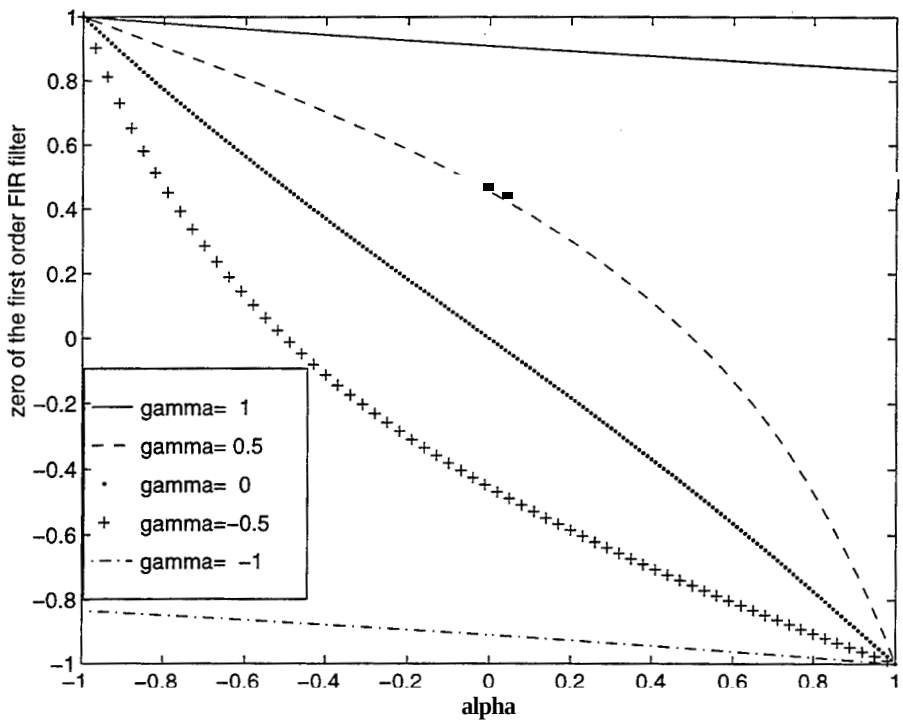

Figure 19. Location of the zero of the first order FIR as a function of the signal and noise correlation coefficients (α and γ) for input signal-to-noise ratio of -10 dB.

Figure 20 shows the location of the zero of the first order FIR filter for y $= -0.5$, and for different values of the input signal-to-noise ratio. The three cases discussed above are again evident from this figure.

1. Processing Gain for First Order Filter.

To obtain an analytical expression for the processing gain defined in (I.29), we first find an expression for the output signal-to-noise ratio (1.31) of the first order FIR filter. Starting with the general expression [Ref. 5]

$$R_y(l) = \sum_{k_0=-\infty}^{\infty} \sum_{k_1=-\infty}^{\infty} R_x(l - k_1 + k_0) h(k_1) h(k_0)$$

and assuming that the signal alone is applied to the filter we have

$$R_{y_s}(0) = \sum_{k_0=0}^{1} \sum_{k_1=0}^{1} R_s(-k_1 + k_0) h(k_1) h(k_0)$$

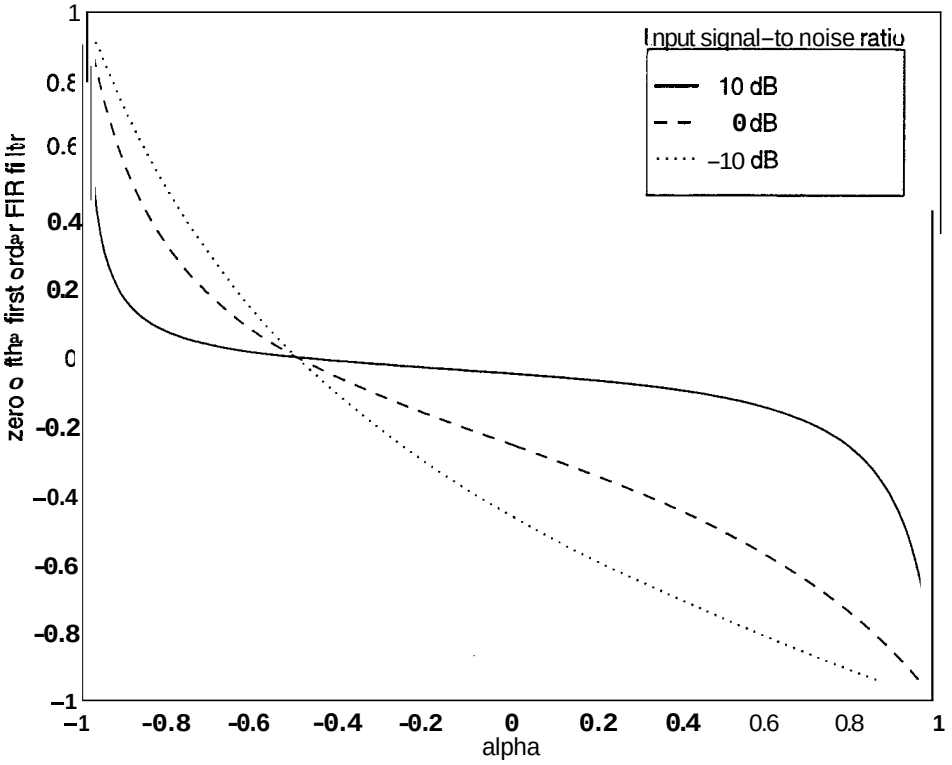

Figure 20. Location of the zero of the first order FIR filter as a function of α for $\gamma = -0.5$, and for different values of the input signal-to-noise ratio

$$= h^2(0)\sigma_s^2\left(\left[\frac{h^2(1)}{h^2(0)}+1\right]+2\frac{h(1)}{h(0)}\alpha\right)$$

and by applying (111.8) we obtain

$$R_{y_s}(0) = h^2(0)\sigma_s^2(z_0^2 - 2z_0\alpha + 1) \tag{111.11}$$

By an identical procedure, we obtain

$$R_{y_\eta}(0) = h^2(0)\sigma_\eta^2(z_0^2 - 2z_0\gamma + 1) \tag{III.12}$$

Finally, by using (111.11) and (111.12) in conjunction with (II.11), (1.29) and (I.31), we can express the processing gain for the first order FIR filter as

$$\boxed{PG = \frac{(z_0^2 + 1 - 2z_0\alpha)}{(z_0^2 + 1 - 2z_0\gamma)}} \tag{111.13}$$

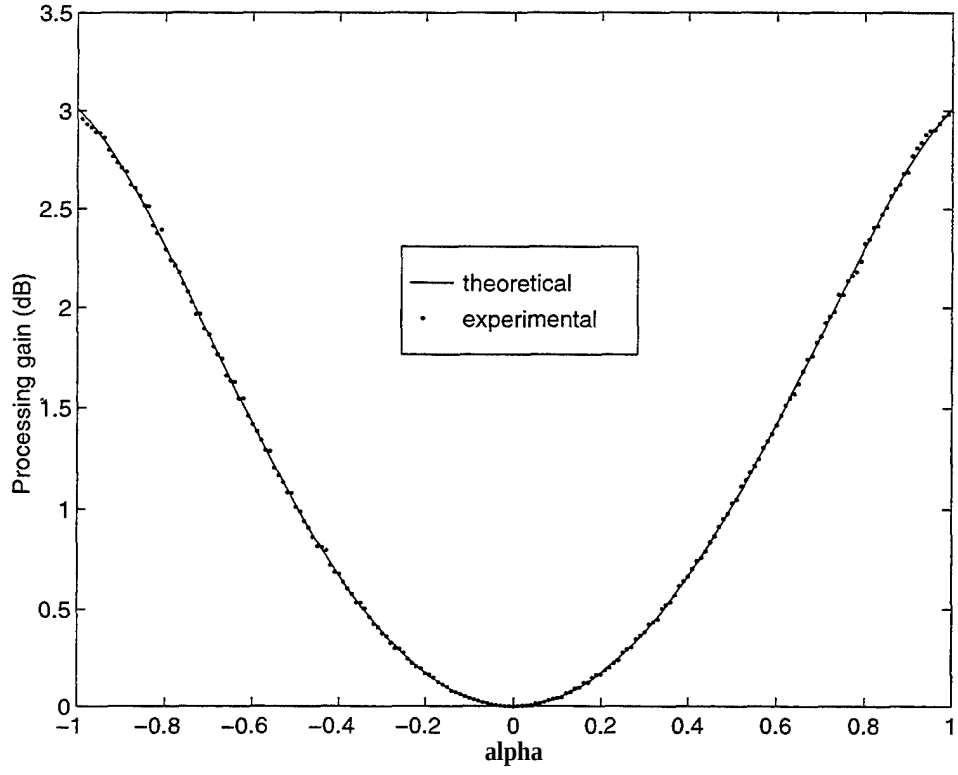

Figure 21. Comparison between the theoretical and experimental values of the processing gain for the first order FIR filter for $\gamma = 0$ (white noise) and input signal-to-noise ratio (ρ_{in}) of 0 dB.

Figures 21 and 22 show that there is good agreement between the theoretical and the experimental values of the processing gain of the first order FIR filter, for the case when y $= 0$ and $\rho_{in} = 0$ dB, and when y $= 0.5$ and $\rho_{in} = -10$ dB, respectively. Figure **23** shows that the processing gain is independent of the input signal-to-noise ratio at three different points. The first point occurs when $a = \gamma$, as mentioned before, when the filter becomes an "all pass" filter; here the resulting processing gain is 0 dB. The other two points occur when $a = \mathrm{f}\,1$ and $\gamma \neq \mathrm{f}\,1$, where $z_0 = \mp 1$, and upon substituting this result into (III.13), we find that the processing gain becomes $PG|_{\alpha=\pm 1} = 2/(1 \pm \mathrm{y})$, i.e., independent of the input signal-to-noise ratio.

Figure 23 also shows the general behavior of the processing gain for the first order FIR filter in the white noise case, for different values input signal-to-noise ratio.

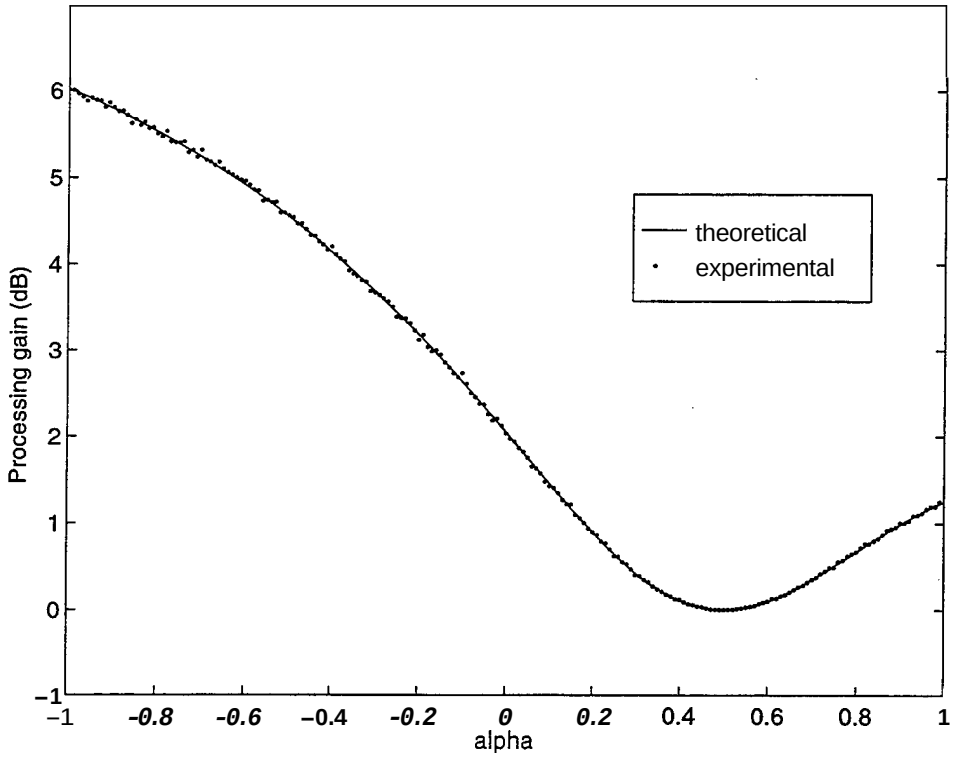

Figure 22. Comparison between the theoretical and experimental values of the processin gain for the first order FIR filter for y = 0.5 (colored noise) and input signal-to-noise ratio (ρ_{in}) of −10 dB.

Notice that higher values of the input signal-to-noise ratio results in lower values of the processing gain. Intuitively, this happens because when the input signal $s(n)$ is strong compared to the noise, the filter cannot make a large improvement. In the limit, as $\rho_{in} \to \infty$ the processing gain goes to zero (except at $\alpha = \pm 1$).

2. Mean Square Error for First Order Filter

The (unnormalized) mean-square error can be computed from (1.14) using (III.3), (III.4), (111.5) and (111.6) yielding

$$\sigma_\epsilon^2 = \boldsymbol{\Theta}, \approx [\sigma_s^2 h(0) + \alpha \sigma_s^2 h(1)]$$

$$= \sigma_s^2 \left[1 - \rho_{in} \frac{\rho_{in} + 1 - \alpha^2 \rho_{in} - 2\alpha\gamma + \alpha^2}{(\rho_{in}+1)^2 - (\alpha\rho_{in} + \gamma)^2} \right] \qquad (111.14)$$

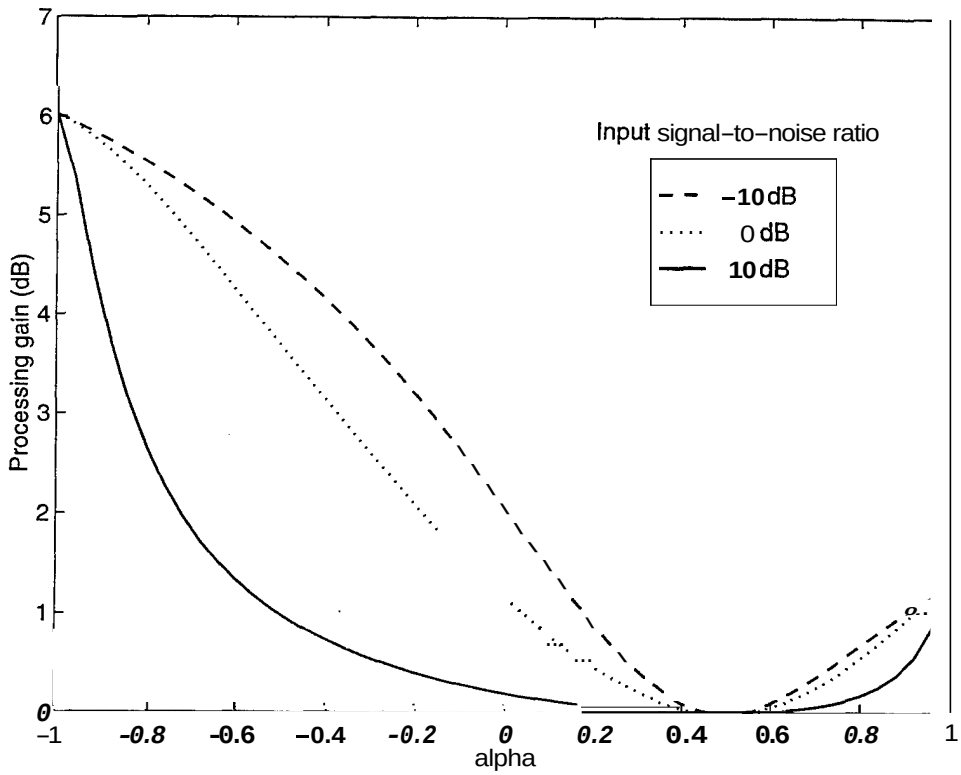

Figure 23. Processing gain for the first order FIR filter as a function of α, for $\gamma = 0$ (white noise), and different input signal-to-noise ratio.

Alternatively, by applying (III.8), it can be written as a function of z_0:

$$\sigma_\epsilon^2 = \sigma_s^2[1 - h(0)[1 - \alpha z_0] \tag{111.15}$$

Using (111.15) in (1.33) gives the normalized mean-square error as

$$\text{MSE} = [1 - h(0)[1 - \alpha z_0] \tag{111.16}$$

Figures 24 and 25 compare the theoretical and experimental values of the normalized mean-square error for different values of input signal-to-noise ratio and the noise correlation parameter γ. Again, there is a good agreement between the theoretical and the experimental curves. Figure 26 shows the behavior of the normalized mean-square error for different values of input signal-to-noise ratio. We see that for higher values of the input signal-to-noise ratio the mean-square error assumes lower values, as expected.

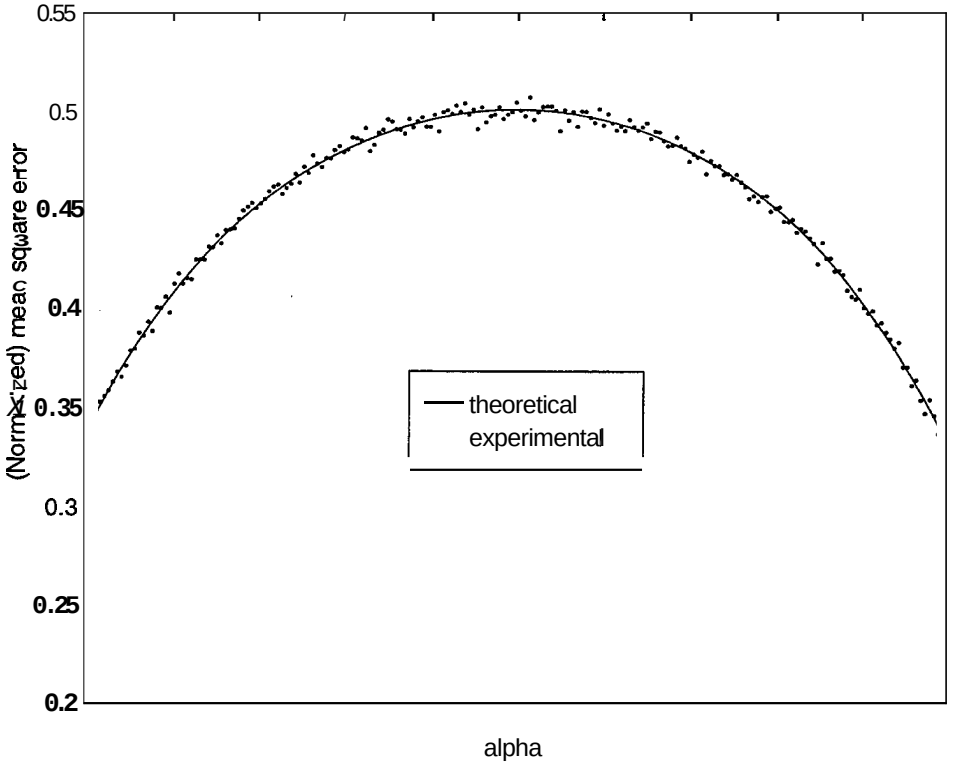

Figure 24. Comparison between the theoretical and experimental values of the mean-square error for the first order FIR filter for $\gamma = 0$ (white noise) and input signal-to-noise ratio of 0 dB.

3. Signal Distortion for First Order Filter

The signal distortion defined by (1.34) is easily evaluated. It is easy to show that the cross correlation between input and output of a linear system is related to the input autocorrelation function by the convolution relation [Ref. 5]

$$R_{xy}(l) = \sum_{k=-\infty}^{\infty} h(k)\ R_x(l-k) \tag{111.17}$$

Hence, for our first order filter we have

$$\begin{aligned} R_{sy_s}(0) &= \sum_{k=0}^{1} h(k) R_s(-k) \\ &= \sigma_s^2 (h(0) + \alpha h(1)) \\ &= \sigma_s^2 h(0)(1 - \alpha z_0) \end{aligned} \tag{111.18}$$

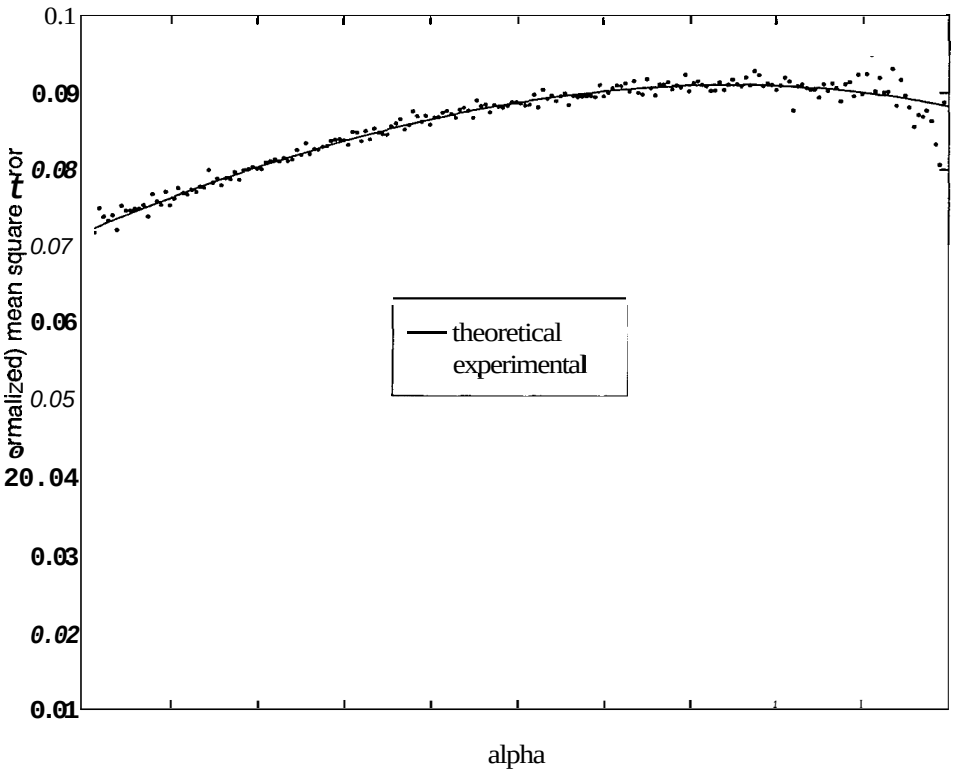

Figure 25. Comparison between the theoretical and experimental values of mean- square error for the first order FIR filter as function of a' for $\gamma = 0.5$ (colored noise) and input signal-to-noise ratio of -10 dB.

Then, by applying (111.18) and (111.11) to (I.34), we obtain

$$\boxed{\mathrm{SD} = \frac{z_0^2(1-\alpha^2)}{1-2\alpha z_0 + z_0^2}} \qquad (111.19)$$

Figure 27 shows the theoretical and experimental values of the signal distortion for different values of α, and for y $= 0$ (white noise) at a input signal-to-noise ratio of 0 dB. We again observe good agreement between the experimental and theoretical results. As in the case of the IIR filter, the distortion is zero for $a' = \gamma$ and $\alpha = \pm 1$, and achieves a maximum value at a point $0 < a', < 1$. In Figures 28 and 29, the noise parameter y has fixed values of 0 (white noise) and 0.5, respectively, and the signal distortion is plotted for different values of the input signal-to-noise ratio. Notice that for lower values of input signal-to-noise ratio the signal distortion assumes higher values. In addition,

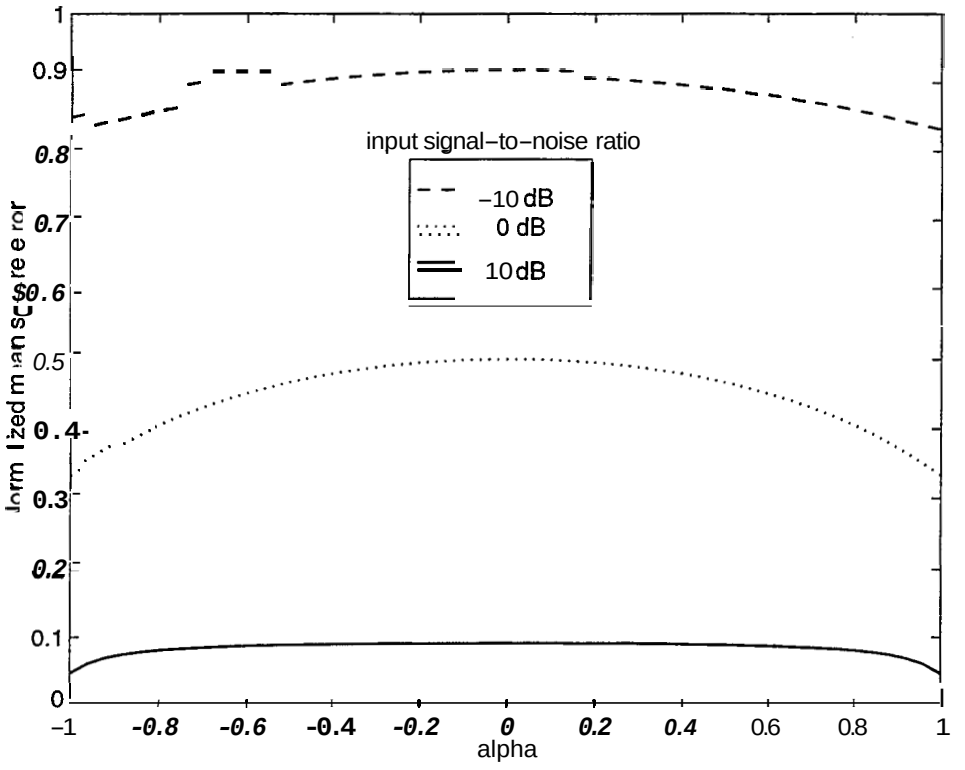

Figure 26. Mean square error for the first order FIR filter as a function of Q for y = 0.5 (colored noise) for different values of input signal-to-noise ratio.

notice that, regardless of the input signal-to-noise ratio, for Q = y or for Q = ±1, the signal distortion is zero. This can also be easily verified from (111.19).

B. PERFORMANCE MEASURES FOR HIGHER ORDER FIR WIENER FILTERS.

For FIR filters of higher than first order $(P > 2)$, it becomes extremely difficult or impossible to derive analytical expressions for the filter coefficients and zeros of the filter in term of the basic parameters Q, y, and ρ_{in}. However it is still useful to be able to compute theoretical values for the processing gain, mean-square error, and signal distortion in these cases. Therefore, in this section we develop a different approach to derive expressions for these performance measures, which can be plotted as a function of the various parameters. With these results, we can compare the performance the FIR

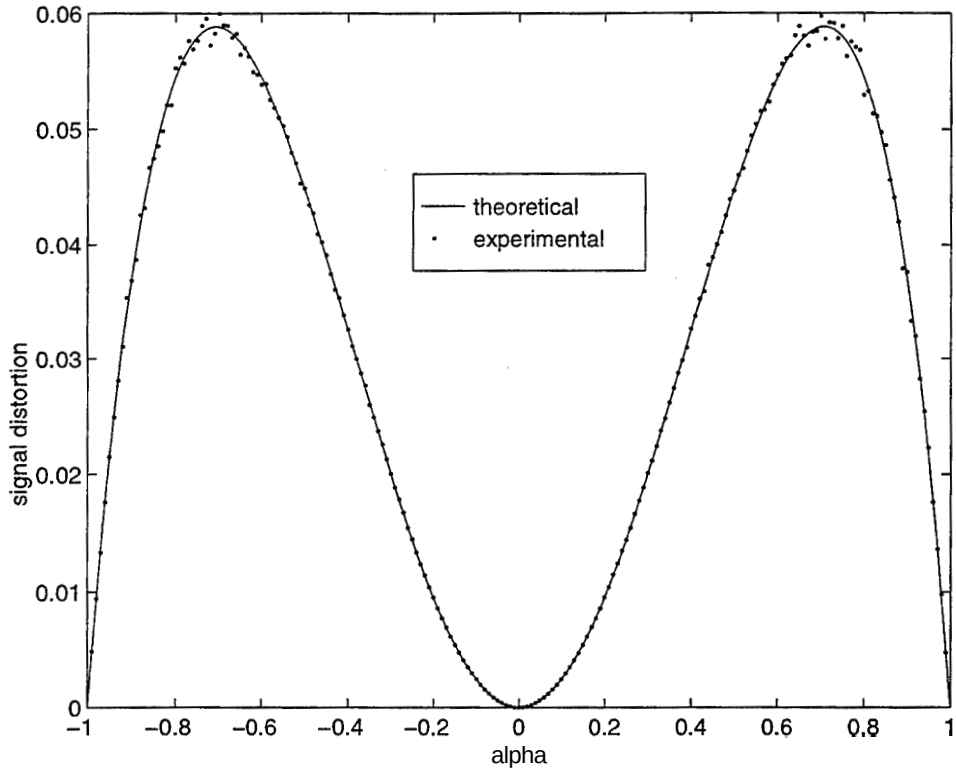

Figure 27. Comparison between the theoretical and experimental values of signal distortion for different values of α and for $\gamma = 0$ (white noise) at a input signal-to-noise ratio of 0 dB.

filter of any order to that of the optimal IIR Wiener filter when they are applied to the first order signal and noise models of equations (1.19) and (1.24).

1. Processing Gain for Higher Order FIR Filter.

The output power of a filter expressed in the form (1.15) can be written as

$$\begin{aligned} R_s(0) &= E\left\{y^2(n)\right\} \\ &= E\left\{(\mathbf{h}^T\tilde{\mathbf{x}})\,(\tilde{\mathbf{x}}^T\mathbf{h})\right\} \\ &= \mathbf{h}^T E\left\{\tilde{\mathbf{x}}\,\tilde{\mathbf{x}}^T\right\}\mathbf{h} \\ &= \mathbf{h}^T\mathbf{R}_x\mathbf{h} \end{aligned} \tag{111.20}$$

Therefore, the output power when the signal and noise act alone is given by

$$R_{y_s}(0) = \mathbf{h}^T\mathbf{R}_s\mathbf{h} \tag{111.21}$$

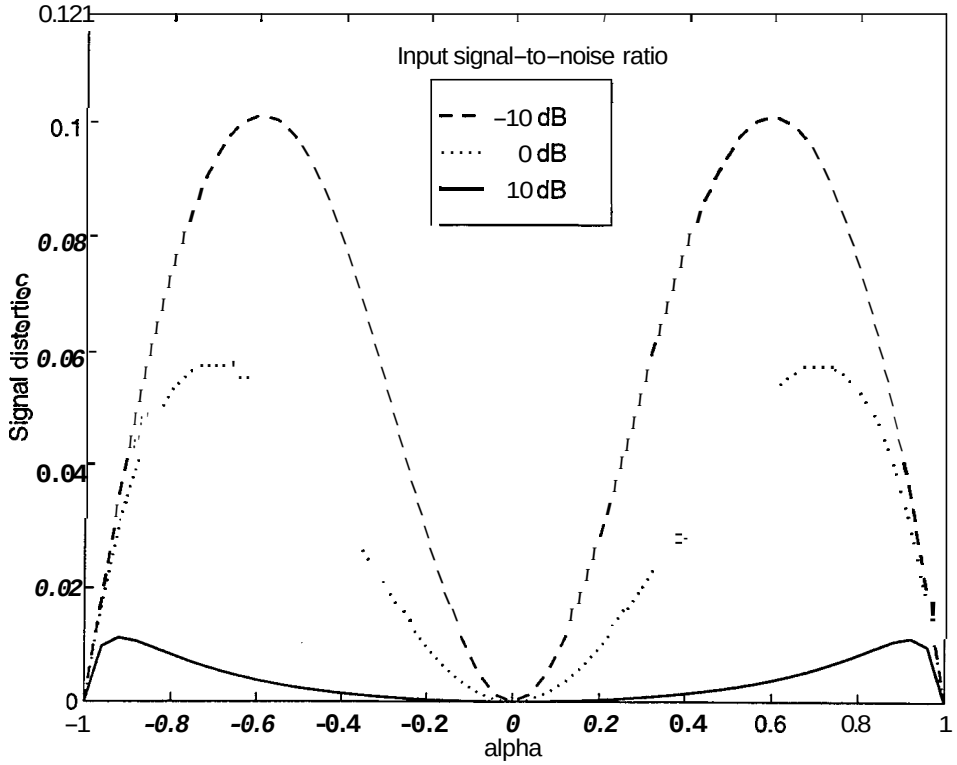

Figure 28. Signal distortion for the first order FIR filter as a function of Q for y = 0 and different values of the input signal-to-noise ratio

and

$$R_{y_\eta}(0) = \mathbf{h}^T \mathbf{R}_\eta \mathbf{h} \tag{111.22}$$

where $\mathbf{R}_s$ and $\mathbf{R}_\eta$ are the signal and the noise correlation matrices, which have the form

$$\mathbf{R}_s = \begin{vmatrix} \sigma_s^2 & \sigma_s^2\alpha & \cdots & \sigma_s^2\alpha^{|P-1|} \\ \sigma_s^2\alpha & \sigma_s^2 & \cdots & \sigma_s^2\alpha^{|P-2|} \\ \vdots & \vdots & \ddots & \vdots \\ \sigma_s^2\alpha^{|P-1|} & \sigma_s^2\alpha^{|P-2|} & \cdots & \sigma_s^2 \end{vmatrix} \quad \mathbf{R}_\eta = \begin{vmatrix} \sigma_\eta^2 & \sigma_\eta^2\gamma & \cdots & \sigma_\eta^2\gamma^{|P-1|} \\ \sigma_\eta^2\gamma & \sigma_\eta^2 & \cdots & \sigma_\eta^2\gamma^{|P-2|} \\ \vdots & \vdots & \ddots & \vdots \\ \sigma_\eta^2\gamma^{|P-1|} & \sigma_\eta^2\gamma^{|P-2|} & \cdots & \sigma_\eta^2 \end{vmatrix} \tag{III.23}$$

Thus from (III.21), (III.22), (1.29) and (1.31) we obtain

$$PG = \frac{\mathbf{h}^T \mathbf{R}_s \mathbf{h}}{\mathbf{h}^T \mathbf{R}_\eta \mathbf{h}} \cdot \frac{1}{\rho_{in}} \tag{111.24}$$

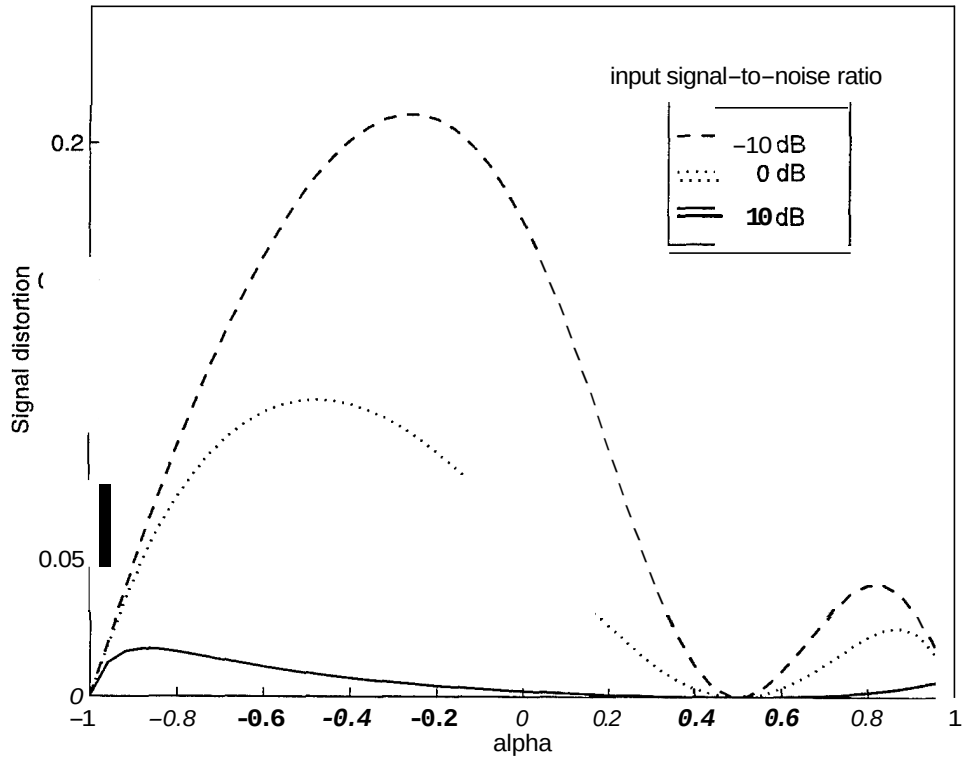

Figure 29. Signal distortion for the first order FIR filter as function of a for y $= 0.5$ and different values of the input signal-to-noise ratio

The processing gain produced by the Wiener filter can be obtained by substituting the solution to the Wiener-Hopf equation (1.16) into (111.24). Specifically, from (1.16) and (1.18) we have

$$\mathbf{h} = (\mathbf{R}, + \mathbf{R}_{\eta})^{-1}\tilde{\mathbf{r}}_s \tag{111.25}$$

Since we have all the necessary expressions, we can plot the values assumed by the processing gain (111.24) for different values of a, y, and ρ_{in}.

Figure 30 shows the behavior of the processing gain as a function of α for y $= 0$ (white noise) and for different values of input signal-to-noise ratio. Notice that the processing gain has different maxima for $\alpha = \pm 1$, depending on the order of the filter. These maximum values can be easily predicted for the white noise case (y $= 0$), as

follows. For $\alpha = 1$ and $\gamma = 0$ the signal and noise correlation matrices (111.23) become

$$\mathbf{R}_s = \begin{bmatrix} \sigma_s^2 & \sigma_s^2 & \cdots & \sigma_s^2 \\ \sigma_s^2 & \sigma_s^2 & \cdots & \sigma_s^2 \\ \vdots & \vdots & \ddots & \vdots \\ \sigma_s^2 & \sigma_s^2 & \cdots & \sigma_s^2 \end{bmatrix} \quad \mathbf{R}_\eta = \begin{bmatrix} \sigma_\eta^2 & 0 & \cdots & 0 \\ 0 & \sigma_\eta^2 & \cdots & 0 \\ \vdots & \vdots & \ddots & \vdots \\ 0 & 0 & \cdots & \sigma_\eta^2 \end{bmatrix} \tag{111.26}$$

Under these conditions (111.25) shows that $h(0) = h(1) = \ldots = h(P-1)$. By applying these results to (111.21) and (III.22), we obtain

$$\mathbf{h}^T \mathbf{R}_s \mathbf{h} = P^2 \, \sigma_s^2 \, h^2(0)$$

and

$$\mathbf{h}^T \mathbf{R}_\eta \mathbf{h} = \sigma_\eta^2 \, P \, h^2(0)$$

Finally, substituting these expressions into (111.24) results in

$$PG = P$$

A similar analysis shows that $PG = P$ also for $a = -1$.

This result shows that unlike the IIR filter, the processing gain for an FIR has a finite bound, which is equal to the filter length. This result can be easily checked in Figure 30 [1]. Notice also that in general, for any value of a, larger length filters produce increased processing gain.

2. Mean Square Error for Higher Order FIR Filter.

The normalized mean-square error (1.33) for any FIR filter is not difficult to obtain. Using (1.15) and (I.1) we can write

$$\begin{aligned} E\left\{(s(n) - y(n))^2\right\} &= E\{(s(n) - \mathbf{h}^T \tilde{\mathbf{s}} - \mathbf{h}^T \tilde{\boldsymbol{\eta}})(s(n) - \tilde{\mathbf{s}}^T \mathbf{h} - \tilde{\boldsymbol{\eta}}^T \mathbf{h})\} \\ &= \sigma_s^2 - 2\,\mathbf{h}^T \tilde{\mathbf{r}}_s + \mathbf{h}^T \mathbf{R}_s \mathbf{h} + \mathbf{h}^T \mathbf{R}_\eta \mathbf{h} \end{aligned}$$

[1] Note that the vertical scale in Figure 30 is in dB

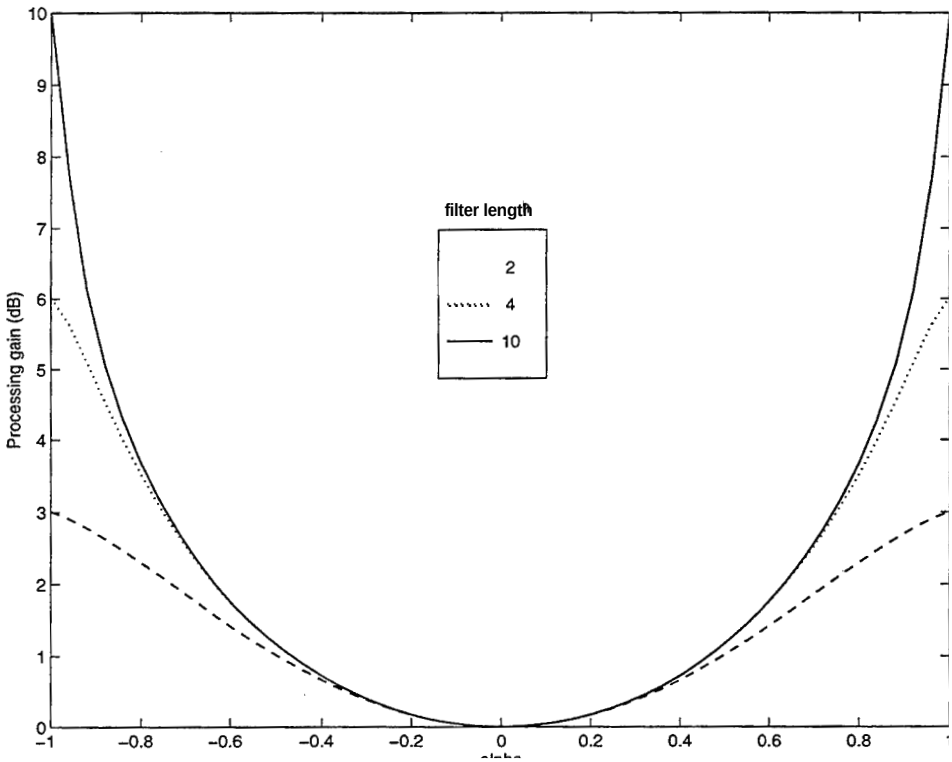

Figure 30. Processing gain for the FIR filter of length P for $\gamma = 0$ (white noise) and input signal-to-noise ratio of 0 dB

where the cross terms disappear because the signal and noise are uncorrelated. Then, substituting this expression in (1.33) we obtain

$$\text{MSE} = 1 - \frac{2\,\mathbf{h}^T \tilde{\mathbf{r}}_s - \mathbf{h}^T \mathbf{R}_s \mathbf{h} - \mathbf{h}^T \mathbf{R}_\eta \mathbf{h}}{\sigma_s^2} \tag{111.27}$$

The result (111.27) applies to any FIR filter. For the Wiener filter we can simplify the expression by noting from (1.16) and (1.18) that

$$(\mathbf{R}_s + \mathbf{R}_\eta)\mathbf{h} - \tilde{\mathbf{r}}_s = \mathbf{0}$$

Therefore, for the Wiener filter (111.27) simplifies to

$$\text{MSE} = 1 - \frac{\mathbf{h}^T \tilde{\mathbf{r}}_s}{\sigma_s^2} \tag{111.28}$$

This result can also be obtained directly using (1.17).

Again, we have all the necessary elements to plot the normalized mean-square error as a function of the model parameters and the input signal-to-noise ratio. Figure 31 shows the normalized mean-square error plotted as a function of a, for y $= 0$ and input signal-to-noise ratio of 0 dB. It can be seen that higher order filters result in lower values of mean-square error, as expected. However, for the longer filters, there is significant improvement in performance only for very high values of the signal correlation parameter a, i.e., the ability to reduce mean-square error depends heavily on the correlation present in the signal.

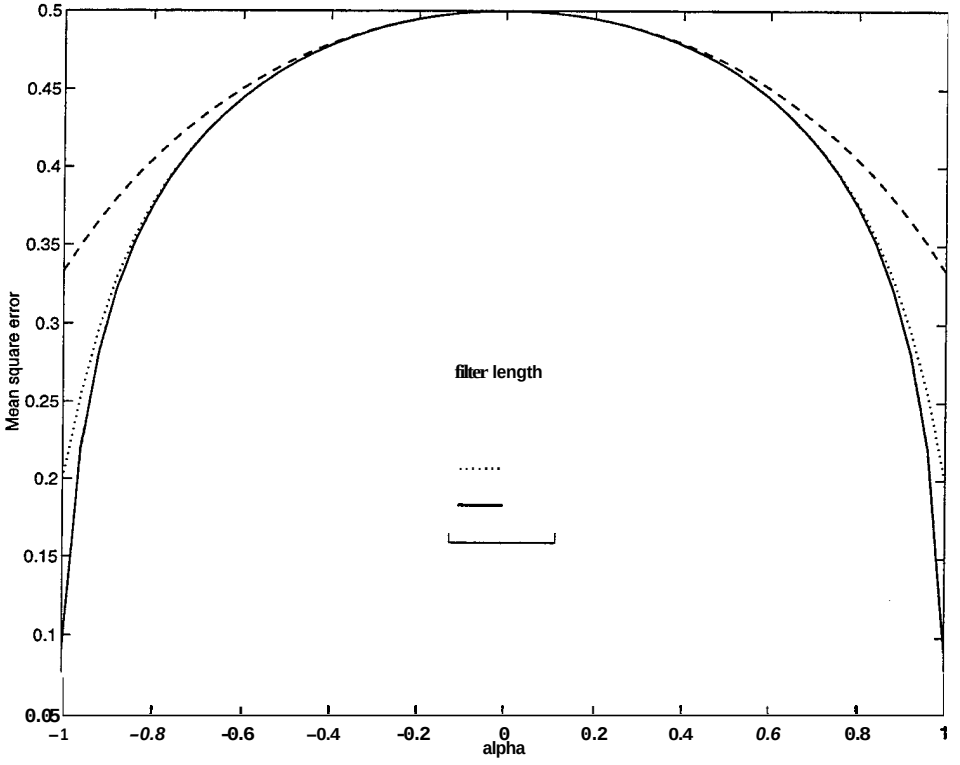

Figure **31.** Mean Square Error for the FIR filter of length P for y $= 0$ (white noise) and input signal-to-noise ratio of 0 dB

3. Signal Distortion for Higher Order FIR Filter.

To derive an expression for the signal distortion for the FIR filter of order P, we write the response of the filter for the signal alone using (1.15) as $y_s(n) = \mathbf{h}^T\ \tilde{\mathbf{s}}$. Thus,

we have

$$E\{s(n)y_s(n)\} = E\{s(n)\ \mathbf{h}^T\ S\} = \mathbf{h}^T\ \tilde{\mathbf{r}}_s \tag{111.29}$$

and

$$E\left\{y_s(n)^2\right\} = E\{\mathbf{h}^T\ \tilde{\mathbf{s}}\ \tilde{\mathbf{s}}^T\ \mathbf{h}\} = \mathbf{h}^T\ \mathrm{R},\ \mathbf{h} \tag{111.30}$$

Substituting these expressions into equation (1.34) then produces the desired expression

$$\mathrm{SD} = 1 - \frac{(\mathbf{h}^T\ \tilde{\mathbf{r}}_s)^2}{\mathbf{h}^T\ \mathbf{R},\ \mathbf{h}} \cdot \frac{1}{\sigma_s^2} \tag{111.31}$$

This can be evaluated for the Wiener filter by substituting the solution (111.25) for h.

Figure 32 shows the behavior of the signal distortion for the FIR filter of different orders P, for $\gamma = 0$ and input signal-to-noise ratio of 0 dB. The behavior of this measure is similar to its behavior in the case of the IIR filter. The signal distortion is 0 dB for $\alpha = \pm 1$ and for $\alpha =$ y and achieves a maximum value around a value $\alpha_\epsilon \approx \pm 0.8$, depending on the length of the filter. In addition, the value of the signal distortion is greater for larger filter lengths.

C. SUMMARY

The analysis carried out in this chapter for the FIR Wiener filter shows that this filter has performance qualitatively similar to that of the IIR filter, although for the case of a first order AR signal and noise model the performance, in terms of the mean-square error and processing gain, is never quite as good.

For the first order FIR filter, which has a single zero, the location of the zero changes from +1 to –1 as the signal correlation coefficient increases from –1 to +1. When the signal and noise have the same correlation coefficient $(a! = \gamma)$ the zero moves to the origin (resultind in an all-pass filter); when both signal and noise are perfectly correlated $(\alpha = \mathrm{y} = \pm 1)$ the zero moves to a location that depends on the input signal-to-noise ratio (see (111.10)). This results in a steady state estimate for the signal which is equal to a constant fraction of the input observation sequence.

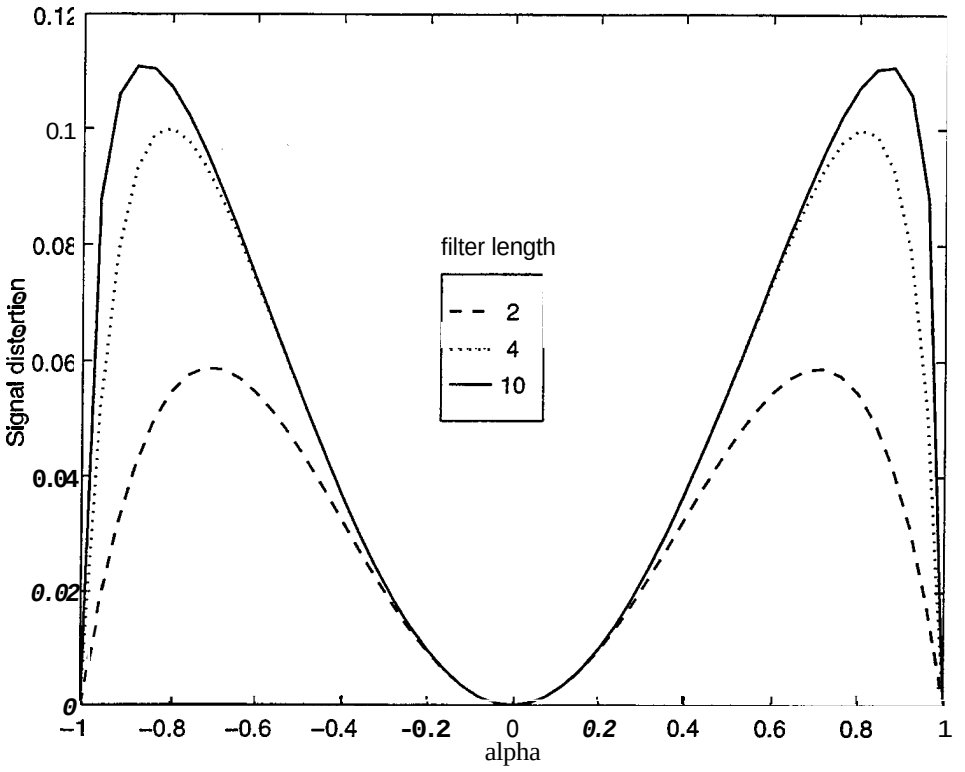

Figure **32.** Signal Distortion for the FIR filter of length P for $\gamma = 0$ (white noise) and input signal-to-noise ratio of 0 dB

The performance measures for the FIR filter approaches those of the IIR filter as the order of the filter increases. Figures 30, 31, and **32** show plots of the three performance measures for the FIR Wiener filter of orders **2, 4,** and 10. These performances can be compared to those for the IIR Wiener filter in Figures **33, 34,** and **35.** **A** significant difference between the two types of filters is that the processing gain of the FIR filter, when the input signal is perfectly correlated is not infinite, but is limited to a value P (the filter length). Also the mean-square error does not go to zero when $a = \pm 1$ as in the IIR filter case. However, the signal distortion for the FIR filter does go to zero for $a = \gamma$ and $a = \pm 1$, as in the IIR filter, and it is not as large as for the IIR filter.

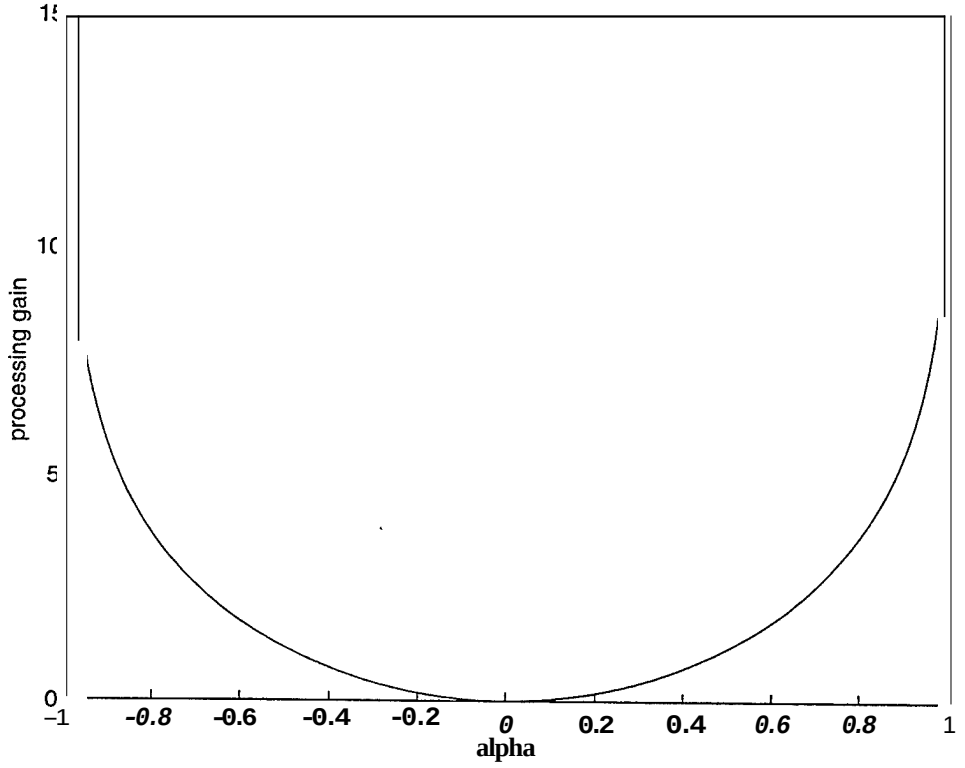

Figure **33.** Processing gain for the IIR filter for $\gamma = 0$ (white noise) and input signal-to-noise ratio of 0 dB

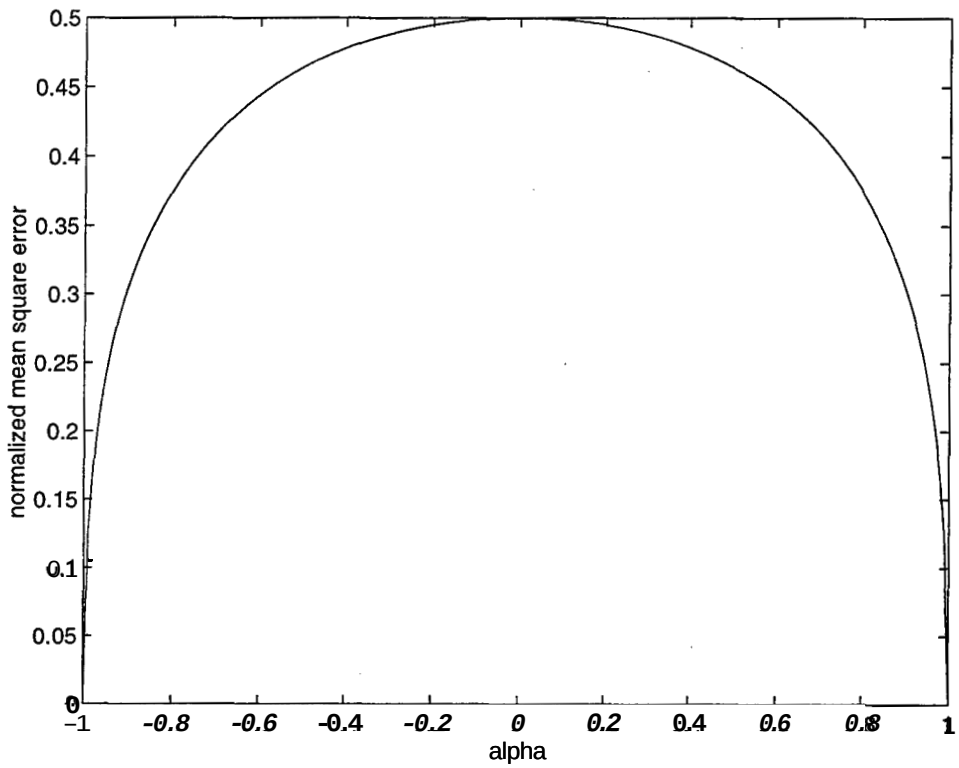

Figure **34.** Normalized mean-square error for the IIR filter for $\gamma = 0$ (white noise) and input signal-to-noise ratio of 0 dB

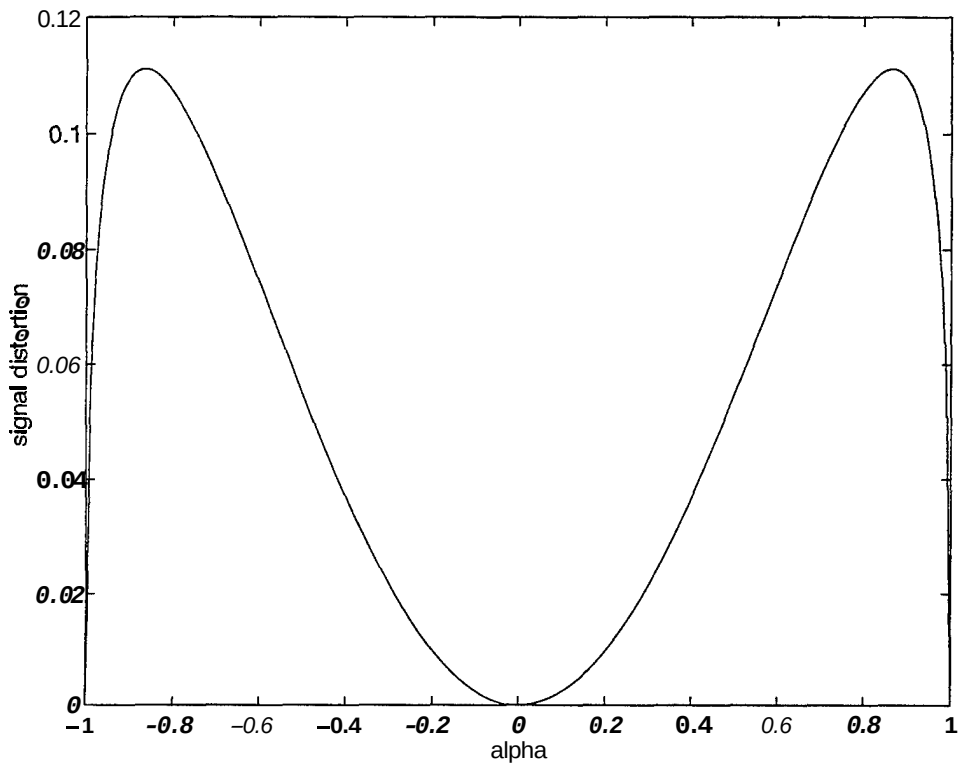

Figure 35. Signal distortion for the IIR filter for $\gamma = 0$ (white noise) and input signal-to-noise ratio of 0 dB

IV. EXTENDED OPTIMAL FILTERING

The results of the previous chapters show that the Wiener filter, although optimal in the mean-square error sense, is not necessarily optimal with regard to minimizing the signal distortion. It will be shown here that is possible to create a whole family of filters related to the Wiener filter where different performance measures are optimized subject to various constraints. We begin with the Wiener filter itself, and then proceed to discuss three possible variations. We then provide an analysis of the performance of the generalized FIR filter for the first order AR signal and noise model, and finally suggest how the generalized filter may be used to obtain an appropriate trade-off between signal distortion and mean-square error.

A. THE EXTENDED OPTIMAL FILTER PROBLEM

1. Minimizing mean-square error

The Wiener filter simply optimizes the mean-square error without any additional constraints. We can derive the FIR form of the filter by beginning with (III.27) which applies to any filter. Then ignoring terms that do not depend on **h,** we can minimize the quantity

$$-2\,\mathbf{h}^T\,\mathbf{I},+\mathbf{h}^T\,\mathbf{R},\,\mathbf{h}+\mathbf{h}^T\,\mathbf{R}_\eta\,\mathbf{h}$$

by taking the gradient with respect to **h** to obtain [Ref. 5: Appendix A]

$$-2\tilde{\mathbf{r}}_s+2\mathbf{R}_s\mathbf{h}+2\mathbf{R}_\eta\mathbf{h}=\mathbf{0}$$

or

$$\mathbf{h}=(\mathbf{R},+\mathbf{R}_\eta)^{-1}\tilde{\mathbf{r}}_s \qquad \text{(IV.1)}$$

which is the Wiener filter. The minimum mean-square error is then given by (111.28).

2. Minimizing distortion with constrained residual noise

Ephraim and Van Trees [Ref. 7] have suggested a more general filter for speech enhancement, based on one measure of the signal distortion. Here we adapt this idea using the signal distortion measure defined in Chapter I.

We begin with the filter depicted in Figure 3, and the responses $y_s(n)$ and $y_\eta(n)$ due to the filter acting on the signal and noise alone. The problem is to minimize the distortion while constraining the residual noise power to satisfy

$$E\left\{y_\eta^2(n)\right\} \leq \sigma_r^2 \tag{IV.2}$$

where σ_r^2 is some chosen level of residual noise power (not less than the mean-square error σ_w^2 for the Wiener filter). We apply this procedure using the signal distortion measure (1.34). In the context of an FIR filter, the problem can be formulated as to minimize (111.31) subject to the constraint

$$E\left\{y_\eta^2(n)\right\} = \mathbf{h}^T\mathbf{R}_\eta\mathbf{h} \leq \sigma_r^2 \tag{IV.3}$$

Let us first consider the procedure for minimizing the signal distortion without the constraint (IV.3). To do this it is necessary to maximize the term

$$\frac{(\mathbf{h}^T\,\tilde{\mathbf{r}}_s)^2}{\mathbf{h}^T\mathbf{R}_s\mathbf{h}} = \frac{\mathbf{h}^T\,\tilde{\mathbf{r}}_s\tilde{\mathbf{r}}_s^T\mathbf{h}}{\mathbf{h}^T\mathbf{R}_s\mathbf{h}} \tag{IV.4}$$

appearing in (111.31). Since the solution is unique only to within a scale factor, this can be done by constraining the denominator to be any constant

$$\mathbf{h}^T\mathbf{R}_s\mathbf{h} = \text{const} \tag{IV.5}$$

and maximizing the numerator. Thus, by forming the *Lagrangian* [Ref. 5, 8]

$$\mathcal{L} = \mathbf{h}^T\tilde{\mathbf{r}}_s\tilde{\mathbf{r}}_s^T\mathbf{h} + \mu(\text{const} - \mathbf{h}^T\mathbf{R}_s\mathbf{h})$$

where μ is a Lagrange multiplier, and setting the gradient of the *Lagrangian* to zero we obtain

$$\nabla_h\mathcal{L} = 2\,\tilde{\mathbf{r}}_s\,\tilde{\mathbf{r}}_s^T\,\mathbf{h} - 2\,\mu\,\mathbf{R}_s\,\mathbf{h} = \mathbf{0}$$

This shows that h must satisfy

$$\tilde{\mathbf{r}}_s \, \tilde{\mathbf{r}}_s^T \, \mathrm{h} = \mu \, \mathrm{R}, \, \mathrm{h} \tag{IV.6}$$

i.e., h is a generalized eigenvector for the two matrices $\tilde{\mathbf{r}}_s \, \tilde{\mathbf{r}}_s^T$ and $\mathbf{R},$. The only non-trivial solution to (IV.6) is given by

$$\mathrm{h} = \mathbf{R}_s^{-1} \, \tilde{\mathbf{r}}_s$$

which is equal to the all-pass filter $\mathrm{h} = [1 \; 0 \; 0 \ldots 0]^T$ with $\mu = \tilde{\mathbf{r}}_s^T \mathbf{R}_s^{-1} \tilde{\mathbf{r}}_s$. Note that the effect of choosing the constant in (IV.5) is merely to multiply the solution by some appropriate scale factor. Since the scale factor is unimportant in this problem, we can assume the constant is chosen so that the unit vector $\mathrm{h} = [1 \; 0 \; 0 \ldots 0]^T$ results.

When we introduce the constraint (IV.3) we need to form a new *Lagrangian*

$$\pounds = (\mathbf{h}^T \tilde{\mathbf{r}}_s) \tilde{\mathbf{r}}_s^T \mathbf{h} + \mu_1 (\mathrm{const} - \mathrm{h}^T \mathrm{R}_s \mathrm{h}) + \mu_2 (\sigma_r^2 - \mathrm{h}^T \, \mathbf{R}_\eta \, \mathrm{h}) \tag{IV.7}$$

where μ_1 and μ_2 are Lagrange multipliers. Setting the gradient to zero then yields

$$\nabla_h \pounds = 2 \, \tilde{\mathbf{r}}_s \, \tilde{\mathbf{r}}_s^T \mathrm{h} - 2 \, \mu_1 \, \mathrm{R}, \, \mathrm{h} - 2 \, \mu_2 \, \mathbf{R}_\eta \, \mathrm{h} = 0$$

or

$$\tilde{\mathbf{r}}_s \, \tilde{\mathbf{r}}_s^T \, \mathrm{h} = \mu_1 (\mathbf{R}_s + \lambda \mathrm{R}_\eta) \mathrm{h}$$

where $\lambda = \mu_2 / \mu_1$. In this case, we see that the solution is given by

$$\boxed{\mathrm{h} = (\mathrm{R}, + \lambda \mathbf{R}_\eta)^{-1} \tilde{\mathbf{r}}_s} \tag{IV.8}$$

with $\mu_1 = \tilde{\mathbf{r}}_s^T (\mathbf{R}_s + \lambda \mathbf{R}_\eta)^{-1} \tilde{\mathbf{r}}_s$. The parameter λ can be related to σ_r^2 through the constraint (IV.2). In particular, substituting (IV.8) into (IV.3) with the equality yields

$$\tilde{\mathbf{r}}_s^T \, (\mathbf{R}_s + \lambda \mathbf{R}_\eta)^{-1} \, \mathbf{R}_\eta \, (\mathbf{R}_s + \lambda \mathbf{R}_\eta)^{-1} \, \tilde{\mathbf{r}}_s = \sigma_r^2$$

which must be solved by iteration. For the case of white noise ($\mathbf{R}_\eta = \sigma_\eta^2 \mathbf{I}$) the equation can be simplified to

$$\mathrm{tr} \, \tilde{\mathbf{r}}_s \, \tilde{\mathbf{r}}_s^T \, (\mathrm{R}, + \lambda \sigma_\eta^2 \mathbf{I})^{-2} = \sigma_r^2 / \sigma_\eta^2 \tag{IV.9}$$

The solution (IV.8) for the extended optimal filter is the same as that of a Wiener filter with modified noise power. Some particular special cases are of interest. For $\lambda = 0$ we obtain the all-pass filter $\mathrm{h} = [1\ 0 \ldots 0]^T$ (as we have already noted), resulting in the maximum residual noise power $\sigma_r^2 = \sigma_\eta^2$ and zero signal distortion. For $\lambda = 1$ we have the Wiener filter which minimizes the residual noise power $\sigma_r^2 = \sigma_w^2$. By choosing an appropriate value $0 \leq \lambda \leq 1$ we obtain minimum distortion with residual noise $\sigma_w^2 \leq \sigma_r^2 \leq a;$.

3. Minimizing distortion for fixed processing gain

For this problem the processing gain (111.24) is constrained to a fixed value

$$\frac{\mathbf{h}^T\mathbf{R}_s\mathbf{h}}{\mathbf{h}^T\mathbf{R}_\eta\mathbf{h}} \cdot \frac{1}{\rho_{in}} = G \tag{IV.10}$$

and it is desired to maximize the term

$$\frac{(\mathbf{h}^T\tilde{\mathbf{r}}_s)^2}{\mathrm{h}^T\mathrm{R}_s\mathrm{h}} = \frac{\mathbf{h}^T\tilde{\mathbf{r}}_s\tilde{\mathbf{r}}_s^T\mathbf{h}}{\mathrm{h}^T\mathrm{R}_s\mathrm{h}}$$

appearing in the signal distortion equation (111.31). Since the solution for h is only unique to within a scale factor, one can introduce the constraint

$$\mathrm{h}^T\mathrm{R}_s\mathrm{h} = \text{const}$$

where as before, the constant can be left unspecified. Then it is desired to maximize the term $\mathbf{h}^T\tilde{\mathbf{r}}_s\tilde{\mathbf{r}}_s^T\mathbf{h}$ subject to the additional constraint

$$\mathbf{h}^T\mathbf{R}_\eta\mathbf{h} = \frac{\text{const}}{G\rho_{in}}$$

We thus form the Lagrangian

$$\mathcal{L} = \mathbf{h}^T\tilde{\mathbf{r}}_s\tilde{\mathbf{r}}_s^T\mathbf{h} + \mu_1(\text{const} - \mathrm{h}^T\mathrm{R}_s\mathrm{h}) + \mu_2(\text{const}/G\rho_{in} - \mathrm{h}^T\mathrm{R}_s\mathrm{h})$$

and set the gradient to zero to obtain

$$2\tilde{\mathbf{r}}_s\tilde{\mathbf{r}}_s^T\mathrm{h} - 2\mu_1\mathbf{R}_s\mathbf{h} - 2\mu_2\mathbf{R}_\eta\mathbf{h} = \mathbf{0}$$

or

$$\tilde{\mathbf{r}}_s\tilde{\mathbf{r}}_s^T\mathbf{h} = \mu_1(\mathbf{R}_s\mathbf{h} + \lambda\mathbf{R}_\eta)\mathbf{h}$$

where $\lambda = \mu_2/\mu_1$. As before, the only nontrivial solution to this generalized eigenvalue problem is given by

$$\mathbf{h} = (\mathbf{R}, + \lambda\mathbf{R}_\eta)^{-1}\tilde{\mathbf{r}}_s$$

which is of the same form as (IV.8). Note that if the constant had been specified in the constraint introduced above, a scale factor would have been required in the last equation. Since the scale factor is unimportant, the solution stands as specified.

In order to find the appropriate value for λ, we can apply the original constraint (IV.10), writing it as

$$\mathbf{h}^T\mathbf{R}_s\mathbf{h} - G\rho_{in}\mathbf{h}^T\mathbf{R}_\eta\mathbf{h} = 0$$

so that λ is the solution to the quadratic equation

$$\mathbf{h}^T(\lambda)\mathbf{A}\mathbf{h}(\lambda) = 0 \qquad \text{(IV.11)}$$

with

$$\mathbf{A} = \mathbf{R}_s - G\rho_{in}\mathbf{R}_\eta \qquad \text{(IV.12)}$$

and $\mathbf{h}(\lambda)$ is given by (IV.8). Note that G must be chosen such that solutions exist and the equation needs to be solved by iteration.

4. Maximizing processing gain with fixed distortion

A final problem considered here is to maximize the processing gain while constraining the distortion to be no more than some fixed value D. For this, the problem is to maximize the term

$$\frac{\mathbf{h}^T\mathbf{R}_s\mathbf{h}}{\mathbf{h}^T\mathbf{R}_\eta\mathbf{h}}$$

subject to the constraint

$$1 - \frac{(\mathbf{h}^T\,\tilde{\mathbf{r}}_s)^2}{\mathbf{h}^T\,\mathbf{R}_s\,\mathbf{h}} \cdot \frac{1}{\sigma_s^2} = D \qquad \text{(IV.13)}$$

Again, the solution is determined only to within an arbitrary scale factor, so we can convert the problem to one of *minimizing* the term $\mathbf{h}^T\mathbf{R}_\eta\mathbf{h}$ subject to the two constraints

$$\mathbf{h}^T\mathbf{R}_s\mathbf{h} = \text{const} \qquad \text{and} \qquad (\mathbf{h}^T\tilde{\mathbf{r}}_s)^2 = (1-D)\sigma_s^2 \cdot \text{const}$$

Expanding the last term and forming the Lagrangian yields

$$\mathcal{L} = \mathbf{h}^T\mathbf{R}_\eta\mathbf{h} + \mu_1(\text{const} - \mathbf{h}^T\mathbf{R}_s\mathbf{h}) + \mu_2((1-D)\sigma_s^2 \cdot \text{const} - \mathbf{h}^T\tilde{\mathbf{r}}_s\tilde{\mathbf{r}}_s^T\mathbf{h})$$

and setting the gradient to zero produces

$$2\mathbf{R}_\eta\mathbf{h} - 2\mu_1\mathbf{R}_s\mathbf{h} - 2\mu_2\tilde{\mathbf{r}}_s\tilde{\mathbf{r}}_s^T\mathbf{h} = \mathbf{0}$$

or

$$\tilde{\mathbf{r}}_s\tilde{\mathbf{r}}_s^T\mathbf{h} = \mu'(\mathbf{R}_s\mathbf{h} + \lambda\mathbf{R}_\eta)\mathbf{h}$$

where $\mu' = -\mu_1/\mu_2$ and $\lambda = -1/\mu_1$. As before, this has the solution

$$\mathbf{h} = (\mathbf{R}_s + \lambda\mathbf{R}_\eta)^{-1}\tilde{\mathbf{r}}_s$$

again of the same form as (IV.8).

The implicit equation for λ can be obtained by writing the constraint (IV.13) as

$$\mathbf{h}^T\tilde{\mathbf{r}}_s\tilde{\mathbf{r}}_s^T\mathbf{h} - \sigma_s^2(1-D)\mathbf{h}^T\mathbf{R}_s\mathbf{h} = 0$$

This is of the same form as (IV.ll) with

$$\mathbf{A} = \tilde{\mathbf{r}}_s\tilde{\mathbf{r}}_s^T - \sigma_s^2(1-D)\mathbf{R}_s$$

The foregoing analyses show that the solution to several problems involves an identical procedure which is equivalent to solving the Wiener filtering problem with a scale factor λ applied to the noise covariance. For each of the problems, this scale factor is determined by solving a different nonlinear equation. We note that not *all* values of

the desired parameter D or G in problems (3) and (4) will lead to legitimate solutions; we must require at least that $0 \leq \sigma_r^2/\sigma_w^2 \leq 1$, $0 \leq G \leq P$, and $0 \leq D \leq 1$. However all values for which the parameter λ is positive lead to correct solutions. Thus, given the form of the optimal filter for these various problems, it is most efficient to start with values of λ and find the appropriate values of residual noise, distortion, or processing gain. An iterative search or table lookup can then be used to find the appropriate value of λ.

In summary, by choosing a value for λ in (IV.8) we can gain more control over the signal distortion at the expense of increased residual noise and mean-square error, or trade off processing gain for lower distortion. In the studies presented below, it is shown that this added flexibility has some definite advantages for noise filtering.

B. PERFORMANCE OF THE GENERALIZED FILTER

By using equation (IV.8) in (111.24) we can study the processing gain of the filter as a function of the parameter λ and the signal correlation coefficient α. Figure 36 shows the results of this computation for $\gamma = 0$ (white noise) and an input signal-to-noise ratio of 0 dB. Notice that the processing gain is lower for lower values of λ, demonstrating that there is less noise removal for $\lambda < 1$.

We can also substitute (IV.8) into equation (111.27) to obtain an expression for the mean-square error as a function of Q and λ. Figure 37 shows these results for the same case as Figure 36, i.e., white noise and an input signal-to-noise ratio of 0 dB. Again, there is decrease in performance for values of $\lambda < 1$, going from minimum mean-square error for $\lambda = 1$, which corresponds to the optimal Wiener filter, to maximum for $\lambda = 0$, which corresponds to an all-pass filter, that does not remove any noise from the observed sequence.

Finally, we can apply (IV.8) to (111.31) and plot signal distortion as a function of α and λ. Figure 38 shows the results for the same case as before. Here we see that the signal distortion of the filter improves for higher values of λ, going from maximum

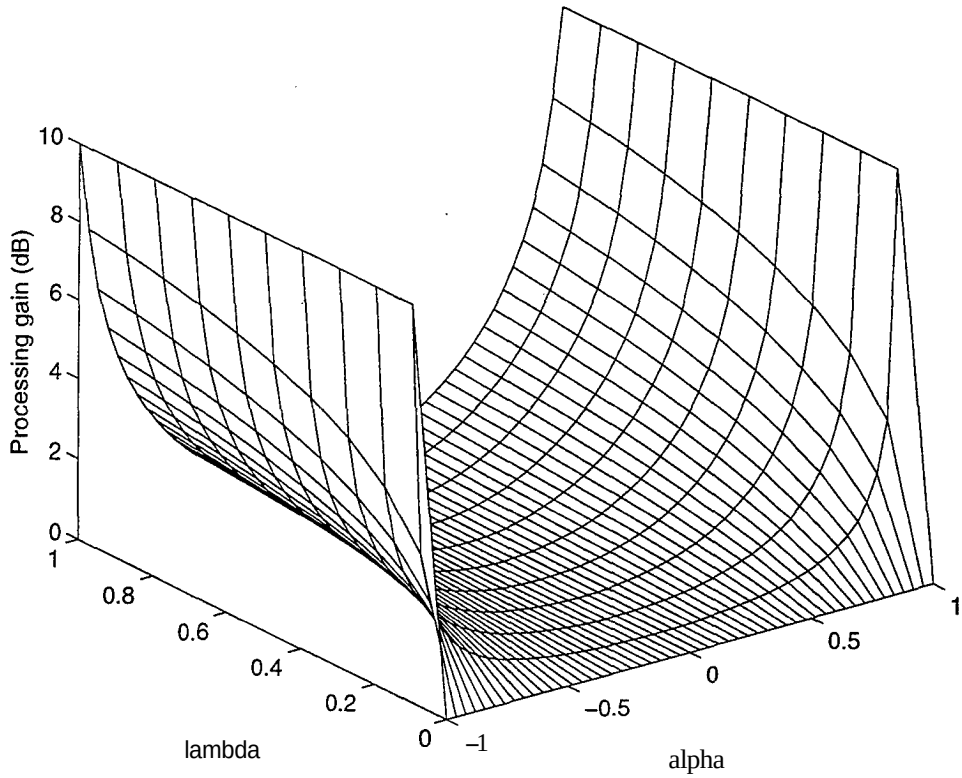

Figure *36.* Processing gain for the generalized Wiener filter as function of α and λ for $\gamma = 0$ (white noise) and input signal-to-noise ratio of 0 dB.

distortion for $\lambda = 1$ (Wiener filter) to minimum distortion for $\lambda = 0$, where the resulting all-pass filter does not alter the signal.

The rate of change of the measures of performance PG, MSE and SD as a function of λ allows one to make useful trade-offs. Notice from Figures **36** through **38** that for values of λ greater than approximately 0.4 the performance of the filter in terms of processing gain and mean-square error does not change significantly, while the signal distortion decreases significantly over this range of values of λ. This implies that the generalized filter with an appropriately chosen value of λ may be more desirable in practical applications involving noise removal than the standard Wiener filter. Since the solution (IV.8) for the filter is equivalent to that of a Wiener filter with an addition parameter, it is convenient to adapt this filter for use in a short-time noise removal algorithm. We will see in the following chapter a practical application of the new algorithm, which provides

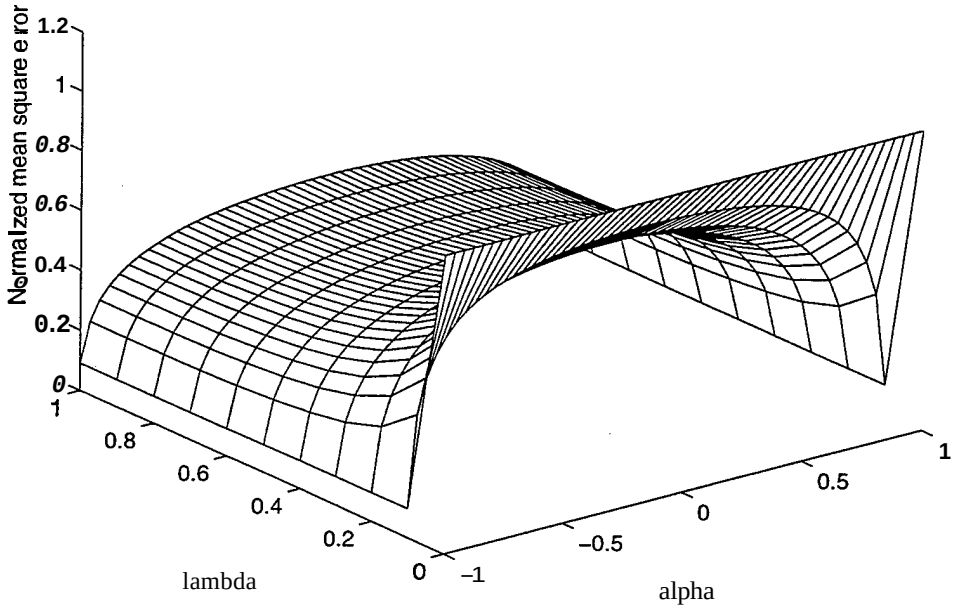

Figure **37.** Mean square error for the generalized Wiener filter as function of α and λ for $\gamma = 0$ (white noise) and input signal-to-noise ratio of 0 dB

good performance and more control over the results.

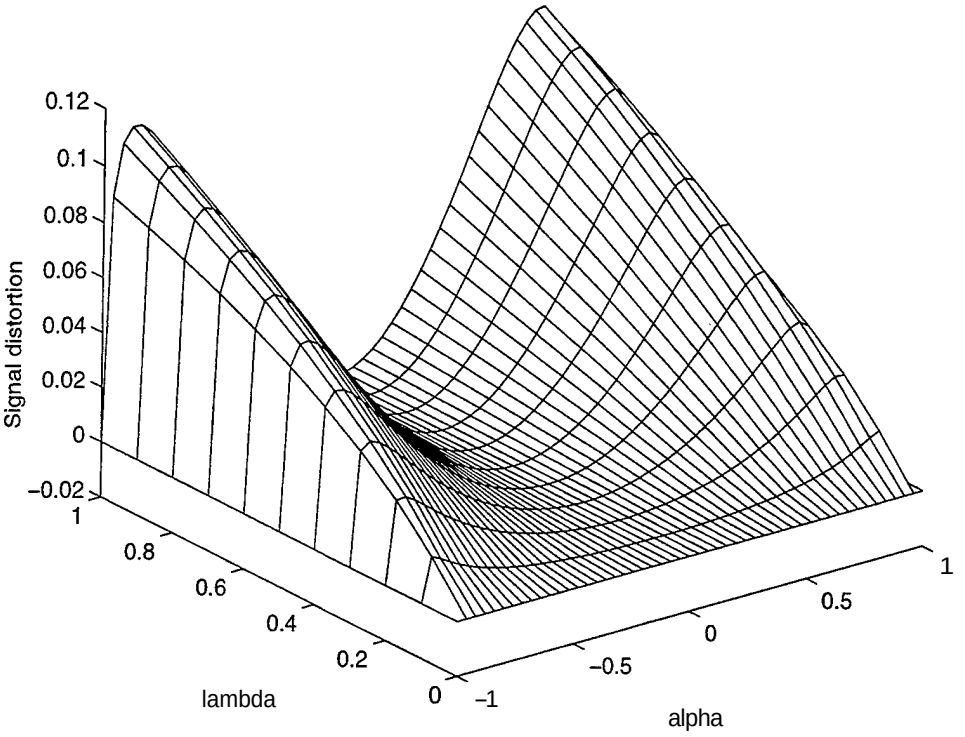

Figure 38. Signal distortion for the generalized Wiener filter as function of α and λ for $\gamma = 0$ (white noise) and input signal-to-noise ratio of 0 dB.

V. APPLYING EXTENDED OPTIMAL FILTERING TO UNDERWATER SIGNALS

A. INTRODUCTION

In this chapter we apply the solution of the extended optimal filter expressed in (IV.8) to the short-time filtering algorithm developed by Frack in [Ref. 4]. This algorithm assumes that both the signal and the noise correlation functions ($R_s(l)$ and $R_\eta(l)$) are unknown a *priori*; therefore they must be estimated from the data at hand. Since only $x(n) = s(n) + \eta(n)$ is observed, however, only $R_x(l)$ can be estimated directly. Nevertheless the nature of the problem provides a way to compute the needed statistics. Since the signal is very short (on the order of seconds or milliseconds) compared to the time over which the noise statistics are likely to change, an estimate for $R_\eta(l)$ can be made from the received data prior to the onset of $s(n)$. By using (I.3), this estimate can in theory be subtracted from $R_x(l)$ to produce an estimate of $R_s(l)$.

Although there is no explicit analytic expression for the parameter λ, we can obtain the value of λ corresponding to any desired residual noise level by solving (IV.9). In the case of white noise, this is equivalent to writing (IV.3) as

$$\sigma_\eta^2 \mathbf{h}^T \mathbf{h} = \sigma_\eta^2 \| \mathbf{h} \|^2 = a_r^2 \tag{V.1}$$

and then (by IV.8) solving for λ from

$$\| (\mathbf{R}_s + \lambda \mathbf{R}_\eta)^{-1} \tilde{\mathbf{r}}_s \|^2 = \frac{\sigma_r^2}{\sigma_\eta^2} \tag{V.2}$$

Therefore, by setting the level of the residual noise σ_r^2 that can be tolerated, we can assign values for λ in each segment by iterating on (V.2) until the equality is satisfied, thus obtaining the value of λ that minimizes the signal distortion. Thus, in principle, all of the quantities to perform the extended optimal filtering over a short time interval can be computed, and this can be repeated over successive blocks of data.

The estimate of $R_s(l)$ by subtraction of the estimated correlation functions is not well formed because there is no guarantee that such an estimate will be positive

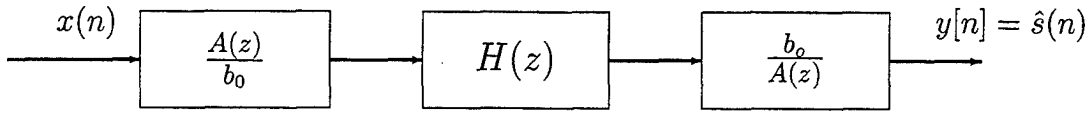

Figure **39.** Prewhitening in Short-Time Extended Filtering Algorithm.

(semi)definite. This problem is mitigated if the noise is white because the procedure then involves subtraction of only a single parameter, the white noise variance, from the estimated R_x at lag zero. Further, the estimate of this single parameter has lower variance than the estimate of the correlation function as a whole. Therefore before any further steps, the entire data set is processed by a linear predictive filter that whitens the noise. After noise removal, the data is processed by the inverse filter as shown in Figure 39.

The prewhitened data is segmented into blocks where an estimate of the local correlation function $R_x(l)$ is formed for each segment. Also, for each segment, the algorithm finds the value of λ, since λ is a function of the $R_s(l), R_\eta(l)$, and σ_r^2. Extended optimal filtering is then performed for each segment using a filter designed for the segment, and the data is processed by the inverse filter to undo the effects of the prewhitening. In performing the filtering, the data is processed both forward and backward through the extended optimal filter. (This gives an approximation to a symmetric noncausal filter of twice the length.) Since the optimal filters are different for each block, discontinuities at the boundaries can arise. The effect of such discontinuities can be minimized by using points from the adjacent segment to filter the early points of the current segment. In the algorithm, the data is actually processed twice. The data is first segmented and filtered and the resulting frames are weighted by a triangular window (see Figure 40). The data is then resegmented using frames shifted by half of the frame length, filtered again and weighted by a triangular window. The two weighted sets of data are then added to produce the final result and minimize any effects that may occur at the boundaries between frames. Additional details of this processing can be found in [Ref. 4].

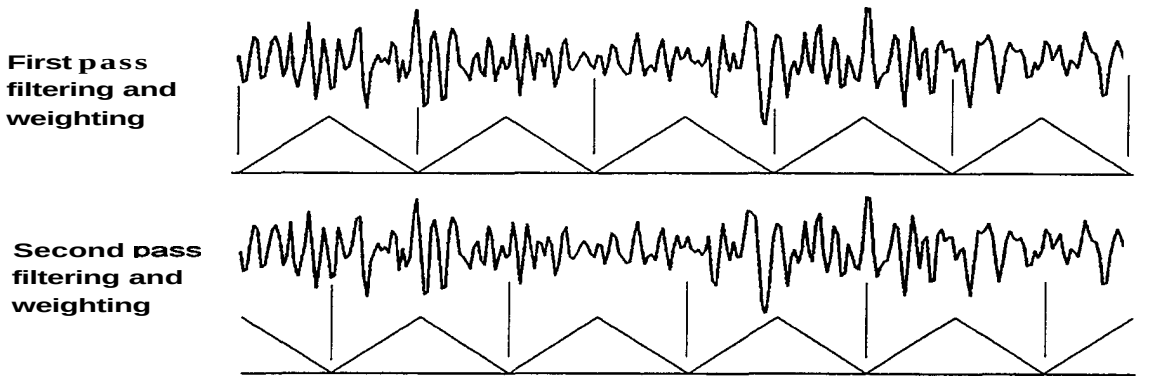

Figure 40. Overlap Averaging Technique Used in Noise Removal.

B. RESULTS

To obtain a quantitative measure of the signal distortion, we first need to have a clean signal $s(n)$, and obtain $y_s(n)$, the response of the filter to this signal $s(n)$, as explained in Chapter I. In this way we can demonstrate our conclusions about the improvement in the signal distortion accomplished by the extended filtering algorithm.

For these experiments, an observation sequence $x(n)$ was generated by adding a white noise sequence with variance σ_w^2 to the clean signal $s(n)$. The sequence $x(n)$ was then processed using the algorithm described above to obtain the filter parameters for each segment of this sequence. These same filter parameters were then used to process the corresponding segments of the clean signal $s(n)$ to obtain $y_s(n)$.

We can now compare the effects of the filter on the signal with respect to signal distortion. In order to do that, we introduce the estimates

$$\widehat{SD} = 1 - \frac{(\sum_n s(n)\ y_s(n))^2}{\sum_n s^2(n)\ \sum_n y_s^2(n)} \tag{V.3}$$

and

$$\widehat{\mathrm{MSE}} = \frac{\sum_n (s(n) - y(n))^2}{\sum_n s(n)^2} \tag{V.4}$$

where the summation is over all points in all segments.

For all the following experiments, the segment (frame) length is 100 points, the filter order is *35,* and the AR model order for the noise was arbitrarily set to 10 (this

parameter could be set to any value since the noise is white). The first 1,000 points data, consisting of noise, was used for the noise sequence.

Figure 41 shows the result of filtering a clean synthetically generated short pulse signal with 1,400 points (41(a)), contaminated by white noise with variance $\sigma_w^2 = 0.36$ (41(b)), using the traditional Wiener filter. The result, shown in Figure 41(c), indicates that the filter is effective in removing the noise. The signal distortion estimate (V.3) for this case is $\widehat{SD} = 0.0556$, and the normalized mean-square error estimate (V.4) is $\widehat{\text{MSE}} = 0.1896$.

Now, by applying the extended filtering algorithm for the case where more residual noise can be tolerated, we can obtain lower signal distortion. Figure 42 shows the graphical results for this case where the residual noise power is set to correspond to 30% of the input noise power ($\sigma_r^2/\sigma_\eta^2 = 0.30$). Part (d) of the figure shows the value of λ that resulted for $\sigma_r^2/\sigma_\eta^2 = 0.30$. Notice that λ assumes values less than 1 for some of the segments. The signal distortion estimate for this case becomes $\widehat{SD} = 0.0541$, which is an improvement of about 3%, and $\widehat{\text{MSE}} = 0.1910$, a degradation of about 0.7%, when compared to the traditional Wiener filtering shown above.

Figure 43 shows the results for an extreme case when the residual noise power is 70% of the input noise power. Here we can see that λ assumes very low values for most of the segments. The signal distortion estimation for this case is very low $\widehat{SD} = .0358$, decreasing the signal distortion by a factor of 36%, and $\widehat{\text{MSE}} = 0.2249$, a degradation of about 18%.

The following table summarizes the results of these experiments using three different settings for the ratio σ_r^2/σ_η^2. The values in parentheses indicate the increase or decrease from the values achieved by the Wiener filter.

The results shown here demonstrate that when more residual noise can be tolerated, the signal distortion produced by the filter decreases significantly while the mean-square error increases by only a modest amount.

The noise removal algorithm was also applied to real underwater acoustic data.

estimates	Wiener Filter	Generalized Filter		
		$\sigma_r^2/\sigma_\eta^2 = 0.3$	$\sigma_r^2/\sigma_\eta^2 = 0.5$	$\sigma_r^2/\sigma_\eta^2 = 0.7$
$\widehat{SD}$	0.0556	0.0541 (−3%)	0.0466 (−16%)	0.0358 (−36%)
		0.1910 (+0.7%)	0.1985 (+5%)	0.2249 (+18%)

Table I. Results from the Generalized Filter Experiments.

Figures 44 and 45 show the results of applying the extended filtering technique to data representing **a** killer whale song. In Figure 44 we used the traditional Wiener filtering process, while in Figure 45 we allowed the residual noise to be 20% of the input noise power. For this case, it is difficult to quantify the performance, since the true underlying signal is unknown. However, upon listening to the signal, the results are at least comparable to those of the Wiener filter and the slight increase in residual noise is the price paid for lower signal distortion.

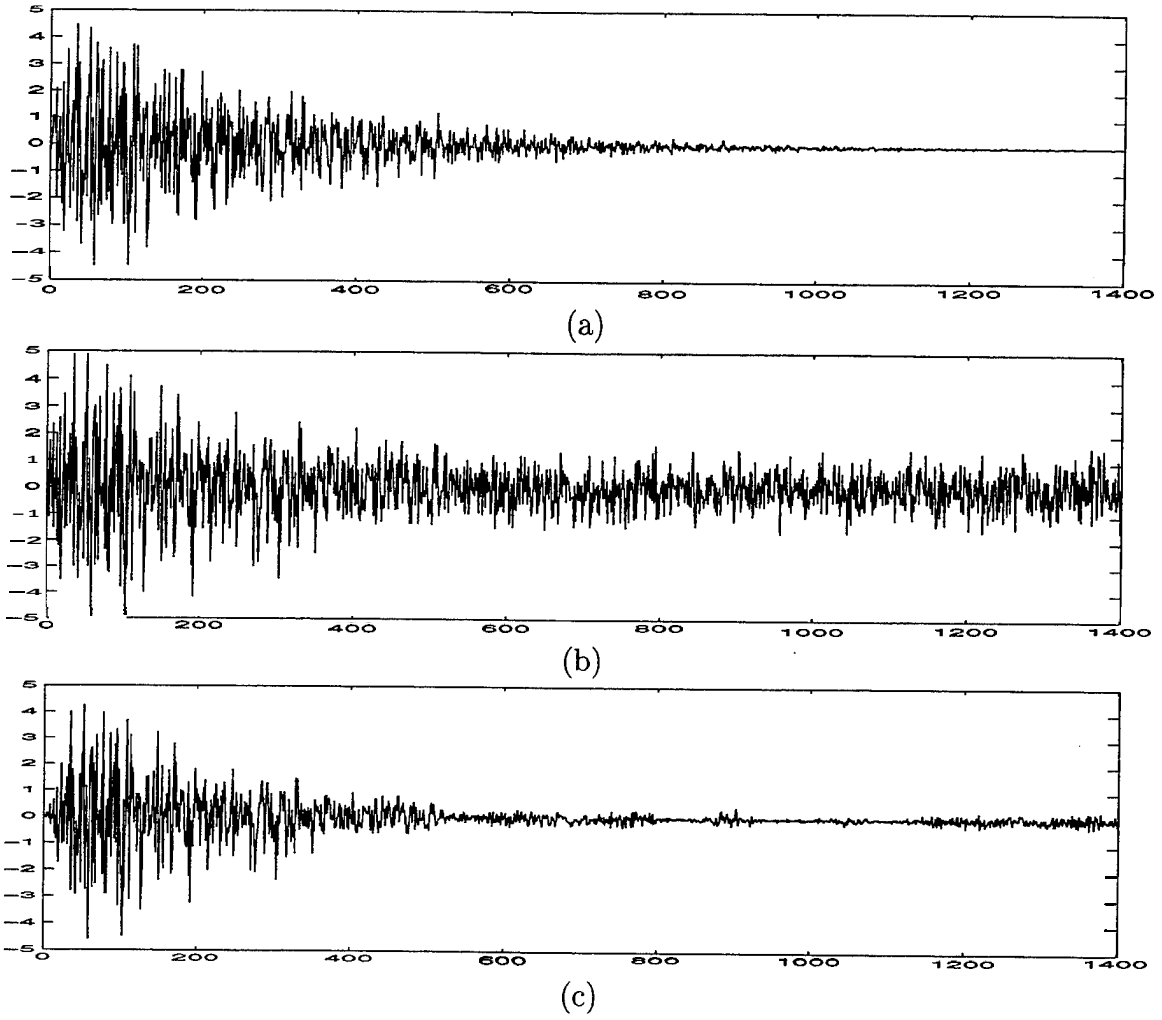

Figure **41.** Results of the Application of the Extended Optimal Filtering Technique to a Synthetically Generated Short Pulse Signal with Added Low Power White Noise, for Minimum Residual Noise ($\lambda = 1$). (a) Original Clean Data. (b) Original Data plus White Noise. (c) Processed Data.

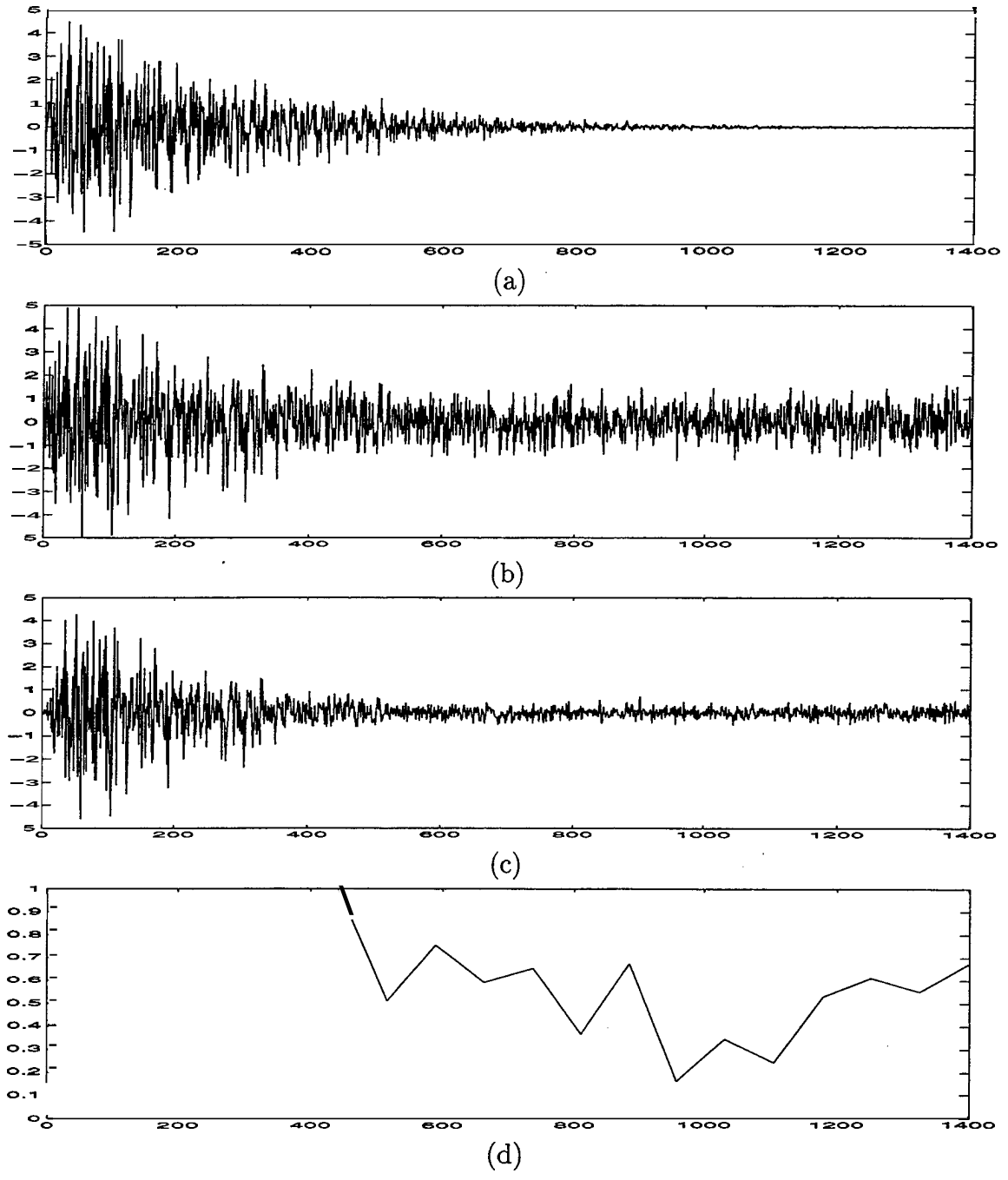

Figure 42. Results of the Application of the Extended Optimal Filtering Technique to a Synthetically Generated Short Pulse Signal with Added Low Power White Noise, for Residual Noise Power Equivalent to 30% of the Input Noise Power. (a) Original Clean Data. (b) Original Data plus White Noise. (c) Processed Data (d) Values of λ for Each Segment.

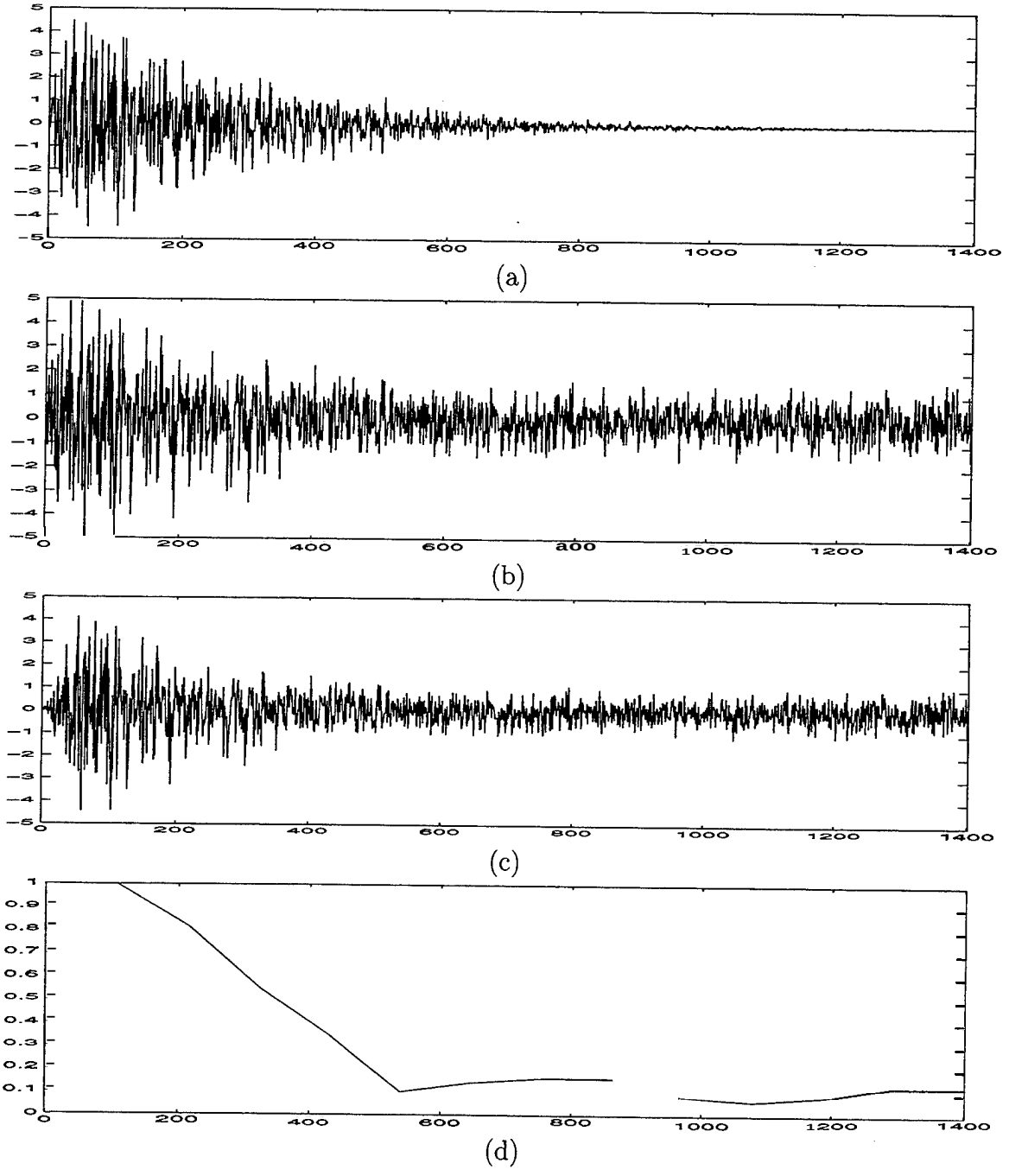

Figure **43.** Results of the Application of the Extended Optimal Filtering Technique to a Synthetically Generated Short Pulse Signal with Added Low Power White Noise, for Residual Noise Power Equivalent to 70% of the Input Noise Power. (a) Original Clean Data. (b) Original Data plus White Noise. (c) Processed Data (d) Values of λ for Each Segment.

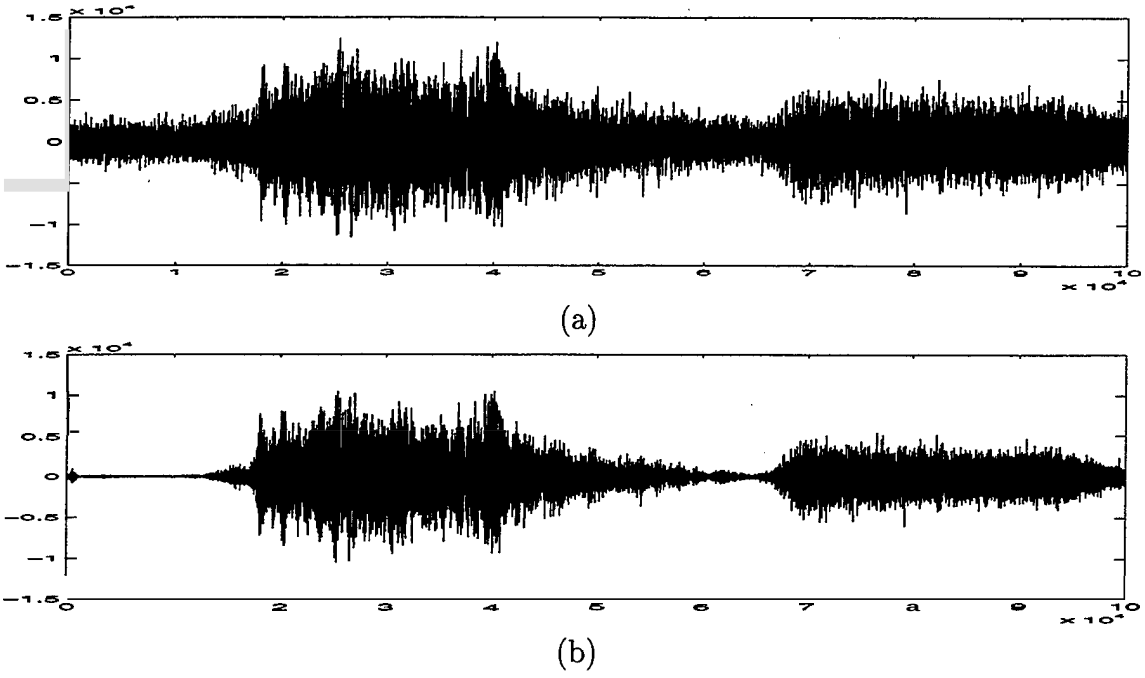

Figure **44.** Results of the Application of the Extended Optimal Filtering Technique to a Killer Whale Song for Minimum Residual Noise ($A = 1$). (a) Original Noisy Data. (b) Processed Data.

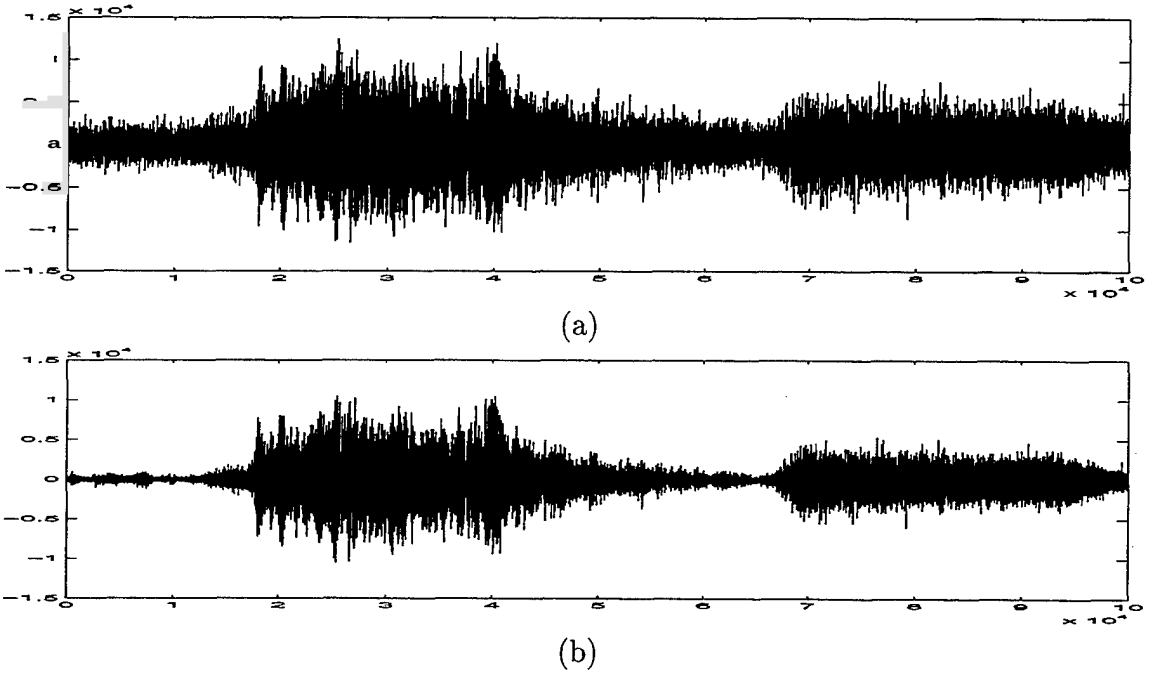

Figure **45.** Results of the Application of the Extended Optimal Filtering Technique to a Killer Whale Song for Residual Noise Power Equivalent to 20% of the Input Noise Power. (a) Original Noisy Data. (b) Processed Data.

VI. CONCLUSIONS

A. SUMMARY

The first three chapters of this report provide an extensive analysis of the IIR and FIR Wiener filters for removing additive noise from a desired signal. Both signal and noise are represented by first order autoregressive (AR) models. Three performance measures, namely processing gain, normalized mean-square error, and signal distortion are defined and evaluated for the Wiener filters based on these models. We believe that the behavior of these filters in terms of the defined performance measures is typical even for other cases with more general signal and noise models.

It was seen that the FIR filter has performance similar to that of the IIR filter, although it does not have the same ideal limiting characteristics such as infinite processing gain when the signal becomes perfectly correlated. We also showed that while both forms of the filter provide lower mean-square error and higher processing gain as the signal becomes more correlated, signal distortion is not a monotonic function of correlation. In particular, the signal distortion for both forms of the filter peaks in a region of moderately high correlation and increases when the input signal-to-noise ratio decreases. This distortion introduced by the filter may be undesirable in some applications.

Chapters IV and V deal with a way to improve the signal distortion resulting from the Wiener filter by considering a more general filtering problem. The result is a generalized solution that can reduce the signal distortion of the Wiener filter, with some increase in the mean-square error and residual noise. This solution was adopted in a short-time filtering algorithm developed by Frack [Ref. 4] and tested. The results illustrate that the extended filter provides more flexibility and allows more control over the signal distortion introduced by the filtering process.

B. FOR FUTHER STUDY

While extensive analytical work is presented in this report, extensive testing of the new algorithms has not been carried out. For example, it would be desirable to carry out formal listening tests to see (over some class of signals) if listeners preferred the results of the generalized filter over those of the conventional Wiener filter or, indeed, if they can hear the difference. The greatest benefits may come in the use of the new algorithms in conjunction with further signal processing steps which may be sensitive to any distortion of the signal introduced by the noise removal process. These are all topics for futher study.

LIST OF REFERENCES

[1] Robert J. Urick. *Ambient Noise in the Sea.* Peninsula Publishing, Los Altos, California, 1986.

[2] F. W. Machell and C. S. Penrod. Probability density functions of ocean acoustic noise processes. In E. J. Wegman and J. G. Smith, editors, *Statistical Signal Processing.* Marcel Dekker, Inc., New York, 1984.

[3] F. W. Machell, C. S. Penrod, and G. E. Ellis. Statistical characteristics of ocean acoustic noise processes. In E. J. Wegman, S. C. Schwartz, and J. B. Thomas, editors, *Topics in Non-Gausian Signal Processing.* Springer-Verlag, New York, 1989.

[4] Kenneth L. Frack, Jr. Improving transient signal synthesis through noise modeling and noise removal. Master's thesis, Naval Postgraduate School, Monterey, California, March 1994.

[5] Charles W. Therrien. *Discrete Random Signals and Statistical Signal Processing.* Prentice Hall, Inc., Englewood Cliffs, New Jersey, 1992.

[6] Norbert Wiener. *Extrapolation, Interpolation, and Smoothing of Stationary Time Series.* The M.I.T. Press (formerly Technology Press), Cambridge, Massachusetts, 1949. (Reprinted as a paperback in 1964.).

[7] Yariv Ephraim and Harry L. Van Trees. A signal subspace approach for speech enhancement. *IEEE Transactions on Speech and Audio Processing,* 3(4):251–266, July 1995.

[8] Gilbert Strang. *Introduction to Applied Mathematics.* Wellesley Cambridge Press, Wellesley, MA, 1986.

INITIAL DISTRIBUTION LIST

		No. Copies
1.	Defense Technical Information Center 8725 John J. Kingman Rd, STE 0944 Ft. Belvoir, VA 22060-6218	2
2.	Dudley Knox Library, Code 52 Naval Postgraduate School 411 Dyer Road Monterey, CA 93943-5101	2
3.	Research Office, Code 09 Naval Postgraduate School 589 Dyer Road Monterey, CA 93943-5138	1
4.	Chairman, Code EC Department of Electrical and Computer Engineering Naval Postgraduate School 833 Dyer Road Monterey, CA 93943-5121	1
5.	Mr. Steven Greineder, Code 2121 Naval Undersea Warfare Center 1776 Howell Street Newport, RI 02841-1706	4
6.	Professor C. W. Therrien, Code EC/Ti Department of Electrical and Computer Engineering Naval Postgraduate School 833 Dyer Road Monterey, CA 93943-5121	4